Journal of Environmental Management 350 (2024) 119659

Contents lists available at ScienceDirect

Journal of Environmental Management

journal homepage: www.elsevier.com/locate/jenvman

Research article

The characteristic of compound drought and saltwater intrusion events in the several major river estuaries worldwide

Dan Li [a], Bingjun Liu [a,b,*], Yang Lu [a], Jianyu Fu [a]

[a] School of Civil Engineering, Sun Yat-sen University, Guangzhou, Guangdong, China
[b] Guangdong Engineering Technology Research Center of Water Security Regulation and Control for Southern China, Sun Yat-sen University, Guangzhou, Guangdong, China

ARTICLE INFO

Handling Editor: Raf Dewil

Keywords:
Drought
Compound event
Estuary
SDSI
Severity

ABSTRACT

Compound Drought and Saltwater intrusion Events (CDSEs) refer to hydrologic drought and saltwater intrusion occurring simultaneously or consecutively in estuaries, and exacerbate the negative impacts resulting from an individual extreme event. CDSEs have been drawing increasing attention due to their potential adverse impacts on water resources, crop production, and food security. A new Standardized compound Drought and Saltwater intrusion Index (SDSI) was developed in this study to systematically detect changes in the severity of CDSEs in six estuaries (Little Back, Ebro, Rhine, Orange, Pearl River and Murray). The results illustrated that (1) compared to the Standardized Runoff Index (SRI), SDSI effectively characterizes and quantifies the occurrences and severity of CDSEs in major river estuaries worldwide. (2) Temporally, the SDSI trend varied across estuaries. Specifically, a decreasing trend was observed in the Little Back, Ebro, and Orange estuaries, with corresponding Zs values of −2.43, −3.63, and −3.23. (3) Spatially, moderate CDSEs occurred more frequently among different estuaries, and their frequency, duration and severity varied in different estuaries. Notably, Ebro, Rhine and Murray River estuaries had the highest probability of CDSEs, nearing 60%. Among them, the Murray Estuary had the longest average duration, spanning 7.68 months, and the highest severity was 5.94. (4) According to the contributions analysis, saltwater intrusion plays a dominant role in influencing SDSI severity, accounting for a substantial percentage (54%–95.30%) compared to runoff. Notably, the Orange Estuary experienced the greatest impact from saltwater intrusion (81.54%–95.30%), while the Murray Estuary had relatively equal contributions from hydrological drought and saltwater intrusion.

1. Introduction

Estuaries, as pivotal transition zones between the river and marine systems, are often located at downstream of rivers, and characterized by high population density and large-scale industrial activities, with substantial demands for freshwater. Additionally, they are vital to coastal ecosystems and communities around the world (Furlan et al., 2021; He et al., 2022; Jia et al., 2021; Zhou et al., 2020). In recent years, there has been a global increase in saltwater intrusion in estuaries, which can be attributed to human activities such as increased upstream freshwater extraction, channel deepening, sand mining, as well as climate change-induced factors like extreme droughts and sea level rise. For instance, Pearl River Estuary in China (Hu et al., 2019; Zhou et al., 2020), Murray Estuary in Australia (Thom et al., 2020; Werner, 2010), Ebro Estuary in Spain (Genua-Olmedo et al., 2016), and Orange River Estuary in southern Africa (Steyl and Dennis, 2010) have all experienced severe saltwater intrusion events. In addition, estuaries are frequently subjected to hydrological droughts and saltwater intrusion, and these two extreme events are interrelated and may occur simultaneously or consecutively (Hao, 2022). The concurrence of prolonged drought and saltwater intrusion in estuary can exert a profound impact on water quantity and quality, adversely affecting drinking water resources, agricultural irrigation, wetland vegetation and aquatic population, and thus imposing significant stress on vulnerable estuarine ecosystems (Conrads and Darby, 2017; He et al., 2018; Jones and van Vliet, 2018). Since the impact of Compound Drought and Saltwater intrusion Events (CDSEs) is often greater than that of individual extreme events, advancing our understanding of the characteristics of such events is of vital importance (Hao, 2022). This will help to mitigate disaster and provide more insightful information for maintaining ecological stability.

Estuaries have complex natural and human environments, because it

* Corresponding author. School of Civil Engineering, Sun Yat-sen University, Guangzhou, Guangdong, China.
E-mail address: liubj@mail.sysu.edu.cn (B. Liu).

https://doi.org/10.1016/j.jenvman.2023.119659
Received 7 August 2023; Received in revised form 22 October 2023; Accepted 18 November 2023
Available online 28 November 2023

Abbreviations full name

CDSEs	Compound Drought and Saltwater intrusion Events
SDSI	Standardized compound Drought and Saltwater intrusion Index
SRI	Standardized Runoff Index
SPI	Standardized Precipitation Index
STI	Standardized Temperature Index
SSI	Standardized Saltwater intrusion Index
KS	Kolmogorov-Smirnov
QQ	Quantile-quantile
PDF	Probability density function
CDF	Cumulative density function
PP	Probability-probability
PMF	Probability multiplication factor
AIC	Akaike Information Criterion
BIC	Bayesian Information Criterion
LOGLIK	Log-likelihood Criteria
USDM	US Drought Monitor
MMK	Modified Mann-Kendall

involves the interaction of topography, sea level, freshwater runoff, water salinity, wind, and other processes, wherein freshwater runoff is a major concern for water managers (Conrads and Darby, 2017; He et al., 2018; Wang et al., 2020a,b,c). Therefore, hydrological drought with runoff deficit incorporates water deficit signals into other hydrological parameters. In general, among all drought types, hydrological drought is highly valued for its fundamental role in water resources management and is also considered to be a thorough drought (Shao et al., 2022; Wu et al., 2019). As a result, numerous indicators have been developed to evaluate hydrological drought in rivers, such as Surface Water Supply Index, Palmer Hydrologic Drought Index, Standardized Runoff Index (SRI), Stream Flow Drought Index, and Standardized Streamflow Index (Karl, 1986; Nalbantis and Tsakiris, 2009; Shukla and Wood, 2008; Vicente-Serrano et al., 2012; Wang et al., 2023). Among them, SRI is regarded as the most prevalent approach to quantifying runoff-based hydrological drought due to its simplicity and effectiveness (Shao et al., 2022; Wang et al., 2020a,b,c). In contrast, water scarcity in estuaries (i.e., hydrological drought) may be caused by the effects of concurrent hydrological drought and saltwater intrusion. Specifically, estuarine hydrologic drought is typically attributed to insufficient upstream runoff that affects estuarine water resources or water supply. At the same time, saltwater intrusion intensifies hydrological drought in estuaries through increasing salinity, thereby reducing water quality and availability, and worsening water supply shortages (Hao, 2022; Wei et al., 2022). Given the complexity of hydrological drought in estuaries, the traditional drought indices, which were developed for upland areas, may not be well suited for describing water shortage caused by hydrological droughts and saltwater intrusion (i.e., CDSEs) in coastal estuaries (Conrads and Darby, 2017). Besides, the coastal salinity index may not accurately reflect drought conditions in estuaries (Mitra and Srivastava, 2021). Consequently, it is necessary to develop a multivariate hydrological drought index that incorporates saltwater intrusion to reliably evaluate water scarcity in estuaries.

Over the past few years, numerous studies have examined multivariate compound events (Li et al., 2021a,b; Zhang et al., 2021; Zscheischler et al., 2020), which were generally identified using either threshold approaches or indicator approaches (Hao et al., 2020; Li et al., 2021a,b). The utilization of thresholds to define the occurrence and frequency of compound extreme events for a specific period has gained considerable attention in recent studies (Wu et al., 2019b; Zhou and Liu, 2018). While this approach has the advantage of visually detecting changes in the occurrence of compound events, it does not provide a comprehensive understanding of the severity and impacts of multiple compound events (Li et al., 2021a,b; Wu et al., 2020). To address these limitations, joint extreme indices have been proposed to transform multivariate compound events into univariate indices, which enables the analysis of more compound event characteristics beyond frequency (Hao et al., 2022; Li et al., 2021a,b). A standardized dry and heat index based on the ratio of marginal probabilities of precipitation and temperature, for example, was employed to measure compound dry and heat events (Hao et al., 2018). Furthermore, a standardized compound event indicator, based on the copula theory that links the marginal distribution of the Standardized Precipitation Index (SPI) and Standardized Temperature Index (STI), has been proposed to assess the severity of compound dry and heat events (Hao et al., 2019a). Such composite indices provide available tools to enhance our comprehension of the frequency, spatial extent and severity of compound dry and heat events (Li et al., 2021a,b). To probe into compound extreme events, previous studies have concentrated on compound dry and heat events, and over the past few decades, some influential hydrometeorological events have also been considered as compound extremes, such as compound drought and saltwater intrusion (Hao, 2022; Wei et al., 2022). Concurrence of hydrological droughts and saltwater intrusion can contribute to urban water shortages, become worse with future sea level rise, and increase the potential risk to estuarine areas under global warming (Hao, 2022; Li et al., 2023). The concurrence of drought and saltwater intrusion, for instance, led to water scarcity in cities such as Zhuhai, Macau, and Guangzhou, and ultimately reduced drinking water supply for around 5 million people in early 2004 (Liu et al., 2019; Shen et al., 2018; Wang et al., 2022c,b,d). The drought in the United States in 2012 affected 22 states and resulted in an estimated $30.3 billion in losses and damages. In coastal areas, the drought and saltwater intrusion into estuaries had further impacts on the environment, economy, and public health (i.e., freshwater supply and shellfish harvesting) (Conrads and Darby, 2017; Mitra and Srivastava, 2021). Despite the severe impact of CDSEs on estuaries, to the author's best knowledge, no studies have yet reported on the development of relevant indices for monitoring compound drought and saltwater intrusion.

When examining hydrological drought in estuaries using the traditional drought index (SRI), the drought characteristics identified tend to be similar to those of runoff distribution. Consequently, salinity distribution is often overlooked, resulting in an incomplete picture of estuary drought characteristics. To address this issue, a compound extreme index was established to monitor and assess the severity of hydrological drought and saltwater intrusion, and to verify its reliability in comparison with univariate indices (SRI and Standardized Saltwater intrusion Index (SSI)), in order to comprehensively investigate the concurrent characteristics of such events. This will provide scientific evidence for relevant risk assessment and management.

2. Study area and data

Previous studies have explored freshwater salinization in different regions as well as trends in estuarine runoff, and found that salinization increased in 57% of the sub-basins, with a significant downward trend in estuarine runoff (Shi et al., 2019; Thorslund et al., 2021). Hence hydrological drought and saltwater intrusion conditions may occur simultaneously in an estuary, negatively impacting the social and ecological systems of the estuary. In this study, we quantified CDSEs in six river estuaries around the world.

The study focuses on estuaries spanning different hydroclimatic and geographical regions. These regions include Little Back in North America, Ebro and Rhine in Europe, Orange in Africa, Pearl River in Asia, and Murray in Australia (Fig. 1). The geographical locations of the six estuaries, as well as the corresponding monitoring stations for runoff and salinity, are clearly marked on the map. Little Back and Rhine estuaries are tide-dominated estuaries, while the remaining four estuaries are river-dominated estuaries (Table 1) (Bittar et al., 2016; Bourman et al.,

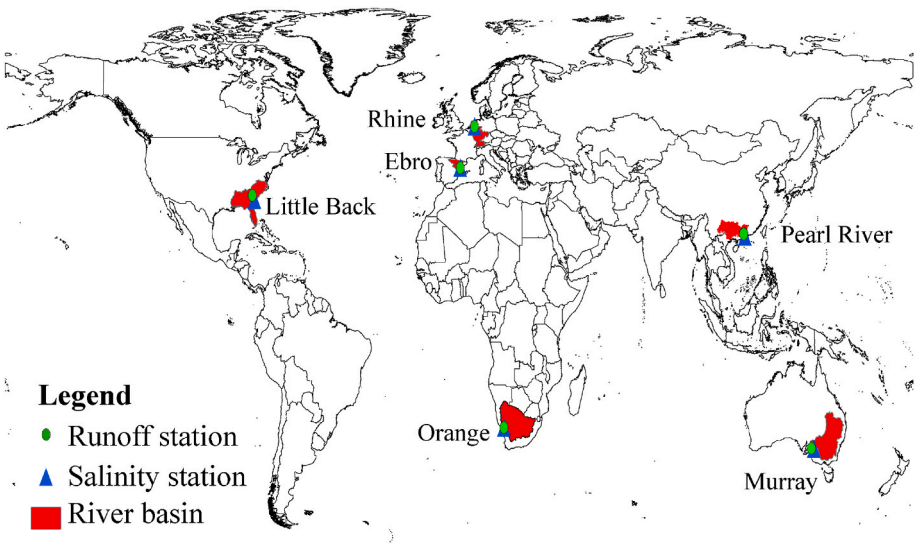

Fig. 1. Locations of the river estuaries used for this study.

Table 1
Statistical characteristics of runoff and salinity data in estuary used in this study.

Estuary	Dominate	Time series	Station	Type	Statistical characteristics			
					Min	Median	Mean	Max
Little Back	Tide-dominated	1994.1–2014.7	USGS-02198500	Runoff (ft^3/s)	4298.33	7431.29	9797.82	42489.29
			USGS-21989784	Salinity (psu)	0.02	0.16	0.20	0.70
Ebro	River-dominated	1980.1–2003.4	GRDC-6226800	Runoff (m^3/s)	64.36	224.02	304.58	1348.80
			ID 300020	Salinity (μS/cm)	412	901	918.62	1593
Rhine	Tide-dominated	1980.1–2009.8	GRDC-6435060	Runoff (m^3/s)	64.36	224.02	304.58	1348.80
			ID 301593	Salinity (μS/cm)	412	901	918.62	1593
Orange	River-dominated	1980.1–2009.12	GRDC-1159100	Runoff (m^3/s)	0.94	67.95	168.29	5328.38
			ID 101888_DWS	Salinity (μS/cm)	202.75	348.75	373.25	819.67
Pearl River	River-dominated	1999–2016 Dry season	Shanshui and Makou	Runoff (m^3/s)	1760	3501.5	4138.31	13,800
			Pinggang	Salinity (mg/L)	5.03	114.88	283.97	2661.1
Murray	River-dominated	1980.1–2009.12	GRDC-5404271	Runoff (m^3/s)	4.53	52.08	146.45	1261.50
			ID w00078_A4260550	Salinity (μS/cm)	214.16	458.09	470.23	1054.23

2022; Codden et al., 2022; Cooper, 2001, 2002; Lu et al., 2022; Nienhuis et al., 2020; Rijnsburger et al., 2021). Little Back Estuary has a humid subtropical climate with an annual precipitation ranging from 1,120 mm to 1,326 mm, and a corresponding annual average temperature ranging from 16.5 °C to 20.9 °C (Ogg et al., 2022). Ebro and Murray estuaries have a Mediterranean climate, which features hot and dry summers, as well as mild and rainy winters. Notably, the rainy and hot seasons in these regions are not concurrent. The Rhine Estuary, situated in Europe, has a temperate maritime climate characterized by mild and humidity conditions, whereas the Orange Estuary has a hot desert climate with limited precipitation and high temperature. Lastly, the Pearl River Estuary has a subtropical monsoon climate characterized by rainfall and heat during the same period, with an annual precipitation ranging from 1,200 to 2,200 mm (Wu et al., 2018).

Within these estuaries, all river monitoring locations have at least 15 years of monthly runoff and salinity data between 1980 and 2020. Specifically, monthly runoff and salinity data for the Little Back Estuary were downloaded from U.S. Geological Survey (https://waterdata. usgs. gov/nwis/rt). The monthly runoff and salinity data for the Pearl River Estuary were obtained from the Hydrological Bureau of Guangdong Province, and those for the Ebro, Rhine, Orange and Murray estuaries were derived from the Global Runoff Data Centre (GRDC, https://www.bafg.de/GRDC/EN/02_srvcs/21_tmsrs/riverdischarge_node.html). Additionally, the corresponding monthly salinity data for these estuaries were derived from previously gathered global salinity dataset (Thorslund et al., 2021). These data were chosen because they also have been used to analyze hydrological drought and freshwater salinization in previous studies (Brunner and Stahl, 2023; Conrads and Darby, 2017; Thorslund et al., 2021; Wada et al., 2013; Zhou et al., 2020). All monthly runoff data used in this study were complete, and all monthly salinity data had a data-missing rate of less than 5%, with missing monthly salinity data replaced by the mean of the same month in each year (Tan et al., 2020, 2022). A summary of the statistical characteristics of all the data used in this study, including the monthly runoff and salinity data for the estuaries (Table 1).

3. Methodology

3.1. Standardized runoff index (SRI) and standardized saltwater intrusion index (SSI)

The SRI was proposed to define and monitor hydrological drought, and has been extensively applied in research into hydrological drought due to its computational simplicity, low input data requirements and applicability to multiple temporal scales (Chen et al., 2018; Valiya Veettil and Mishra, 2020; Vicente-Serrano et al., 2012). To more precisely characterize hydrological drought, five distribution functions (Lognorm, Logistic, Normal, Gamma and Weibull) were utilized to fit the monthly runoff, and the optimal distribution parameters for the monthly runoff data were derived using the maximum likelihood estimation method (Wang et al., 2022a). The Kolmogorov-Smirnov (KS) test was adopted to evaluate the fitting results after the distribution of monthly

runoff data was fitted. The optimal distribution function was then chosen using the smallest statistic of KS test (Wang et al., 2022b; Zhang et al., 2021). Once the optimal distribution and its estimation parameters were determined, the optimal distribution function was then transformed to SRI using the standard normal distribution (Vicente-Serrano et al., 2012). The computational process is as follow:

Based on the optimal probability distribution functions and parameters, the cumulative density function $f(x)$ can be calculated using the following the integral equation.

$$f(x) = \int_0^x f(x)dx \tag{1}$$

Once $f(x)$ was determined, the SRI can be computed by converting $f(x)$ to a standard normal distribution.

$$SRI = k\left(\omega - \frac{\alpha_0 + \alpha_1\omega + \alpha_2\omega}{1 + \beta_1\omega + \beta_2\omega + \beta_3\omega^3}\right) \tag{2}$$

where

$$\begin{cases} \omega = \sqrt{-2\ln(f(x))}, \text{if } f(x) \leq 0.5, \text{then } k = -1 \\ \omega = \sqrt{-2\ln(f(x))}, \text{if } f(x) > 0.5, \text{then } k = 1 \end{cases} \tag{3}$$

where the constants are $\alpha_0 = 2.515517$, $\alpha_1 = 0.8023853$, $\alpha_2 = 0.01328$, $\beta_1 = 1.432788$, $\beta_2 = 0.189269$, $\beta_3 = 0.001308$, respectively.

Similarly, the SSI was calculated in the same process as SRI, except that high values of SSI suggest saltwater intrusion conditions. For consistency and comparability with existing standard drought indices, the SSI values were multiplied by −1 to enable negative values of SRI and SSI to present drought conditions and saltwater intrusion conditions, and positive values of SRI and SSI to present wet conditions and freshwater conditions. And this study is focused on the one-month scale SRI and SSI.

A smaller value of the KS test indicates a better fit. Based on the statistical values, the Lognormal distribution was found to be the optimal function for fitting runoff at all stations (Table 2). This result confirms that the Lognormal distribution is effective in fitting runoff and is consistent with previous research findings (Shukla and Wood, 2008; Vicente-Serrano et al., 2012; Wu et al., 2019). For the distribution of saltwater intrusion, the five distribution functions vary significantly across different estuaries. For instance, the Weibull distribution was found to be suitable for fitting Little Back, and Pearl River estuaries, while the Lognormal distribution to be suitable for fitting Rhine and Orange estuaries. The Gamma distribution was found to be suitable for fitting Ebro and Murray estuaries. Furthermore, the quantile-quantile (QQ), probability density function (PDF), cumulative density function (CDF), and probability-probability (PP) diagrams are utilized to intuitively compare the optimal distribution functions of runoff and saltwater intrusion in both the Pearl River and Little Back estuaries (Fig. 2). For example, the PP plot comparing runoff and salinity data obtained from the Pearl River and Little Back estuaries, and Lognormal distribution function for runoff and Weibull for salinity are almost identical with observations (Fig. 2 (a4, b4, c4, d4)), indicating that these distribution functions fit the runoff and salinity data of these two estuaries well, and can be used to calculat SRI and SSI. In a similar vein, the optimal distribution functions were determined to be used in the calculation of SRI and SSI for each estuary.

3.2. Concurrent drought and saltwater intrusion indicators

CDSEs were defined by runoff deficit (low SRI) and saltwater intrusion (low SSI) over the same period. Three types of composite indicators were introduced in this study, where the percentile-based method and the probability multiplication factor (PMF) method were utilized to validate SDSI. The first indicator is the SDSI, where the focus is on the CDSEs under hydrological drought and saltwater intrusion conditions. Given that copulas have good capability for constructing the joint distribution of multivariate random variables, the joint probability of concurrence of two random variables X (runoff series) and Y (salinity series) based on copula can be expressed as:

$$P(X \leq x \wedge Y > y) = P(X \leq x) - P(X \leq x \wedge Y \leq y) = u - C(u, v) \tag{4}$$

where $u = P(X \leq x), v = P(Y \leq y), C(u, v)$ is the copula function $P(X \leq x \wedge Y \leq y)$.

The joint probability $P(X \leq x \wedge Y > y)$ was then transformed to a uniform distribution by fitting a distribution F (Hao et al., 2019a). The SDSI can be expressed as:

$$SDSI = \Phi^{-1}[F(P(X \leq x \wedge Y > y))] \tag{5}$$

where Φ^{-1} is the inverse function of the standard normal distribution.

Based on the optimal fit of marginal distribution functions for runoff and salinity data, five candidate copula functions were chosen to construct the compound drought and saltwater intrusion model for the estuary. The selection of Copula functions was based on Akaike Information Criterion (AIC), Bayesian Information Criterion (BIC), and Log-likelihood criteria (LOGLIK), and the goodness of fit for the selected Copula functions was evaluated based on the smallest AIC and BIC values and the largest LOGLIK value (Table 3). In general, the selection of the optimal copula function varied across estuaries. In accordance with the optimal marginal distribution functions for runoff and salinity, for instance, the Frank copula was considered to be the optimal joint function for three estuaries (i.e., Little Back, Orange and Pearl River), whereas the Gaussian copula was the optimal joint function for the Murray Estuary. For the Ebro and Rhine estuaries, the optimal joint function for runoff and salinity was the Clayton and Gumbel copula. Based on the optimal copula functions for runoff and salinity in each estuary, the SDSI was constructed. The connection between SDSI and normal distribution was observed in each estuary, with the scatter points were practically located along a straight line, indicating that SDSI can be well-fitted by a normal distribution (Fig. 3).

According to the categories of compound events proposed by Wu et al. (2020), five categories of drought and saltwater intrusion conditions were identified: abnormal, moderate, severe, extreme, and exceptional drought and saltwater intrusion condition, and the same

Table 2
Goodness of fit for marginal distribution functions of monthly runoff and salinity (bold letter indicates minimum values).

Name	Distribution	Little Back	Ebro	Rhine	Orange	Pearl River	Murray
Runoff	Lognorm	**0.12**	**0.07**	**0.06**	**0.06**	**0.08**	**0.12**
	Logistic	0.20	0.15	0.08	0.25	0.13	0.26
	Gamma	0.20	0.09	0.07	0.36	0.11	0.22
	Weibull	0.18	0.09	0.10	0.08	0.14	0.14
	Normal	0.21	0.15	0.13	0.32	0.18	0.28
Salinity	Lognorm	0.10	0.07	**0.04**	**0.05**	0.10	0.05
	Logistic	0.13	0.08	0.06	0.08	0.27	0.07
	Gamma	0.10	**0.07**	0.05	0.06	0.14	**0.05**
	Weibull	**0.08**	0.09	0.09	0.10	**0.07**	0.07
	Normal	0.14	0.09	0.08	0.09	0.26	0.08

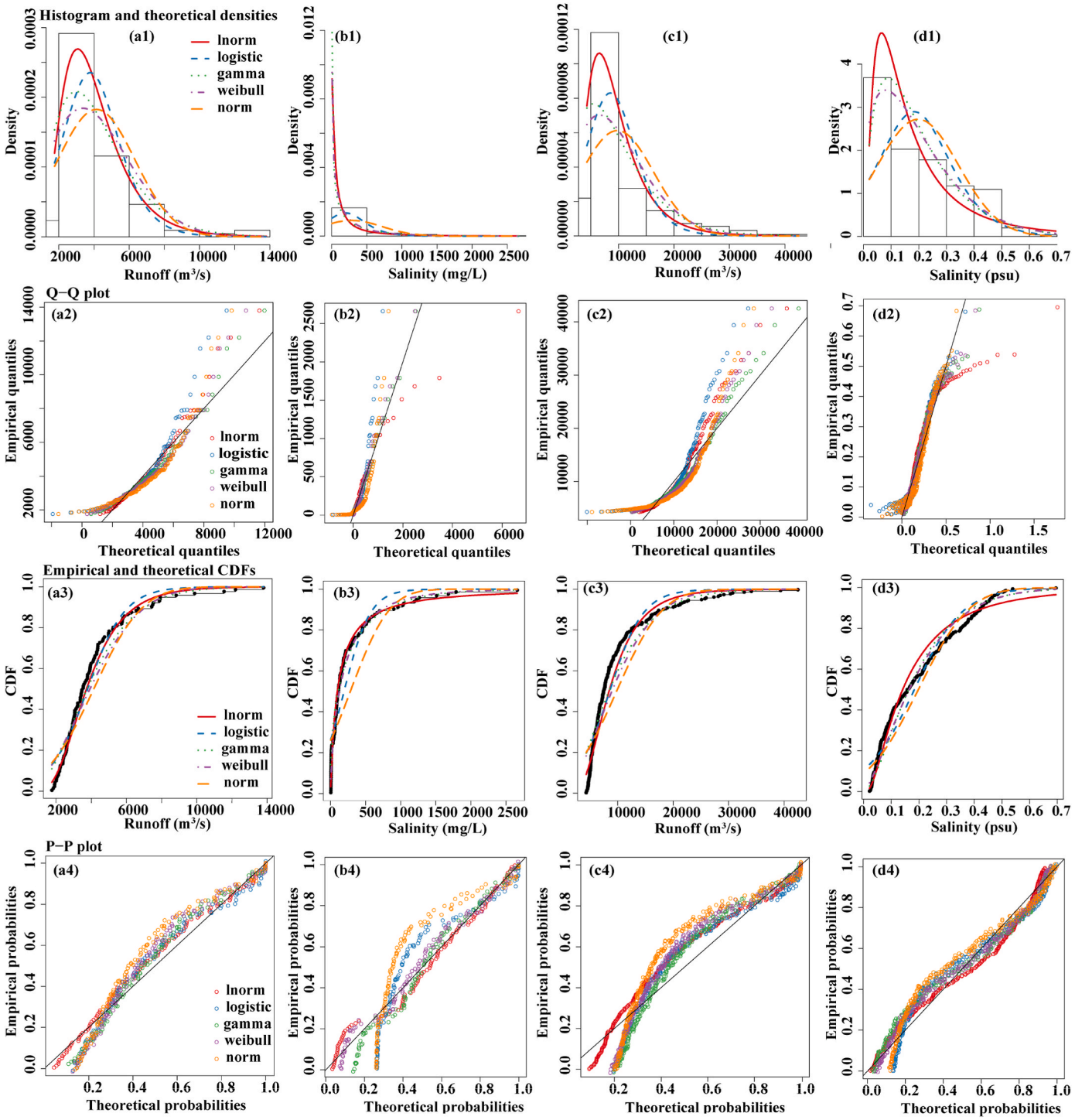

Fig. 2. PDF, QQ, CDF and PP plots of five probability distribution functions (Lognormal, Logis, Gamma, Weibull and Normal) for runoff and salinity in Pearl River (a, b) and Little Back (c, d) estuaries.

criteria were used for SRI and SSI (Table 4). These categories were similar to the severity levels of drought adopted in the US Drought Monitor (USDM) (Svoboda et al., 2002). The fundamental framework of the USDM was based on a ranking percentile approach derived from statistical data. This approach provides historical context for a given value/score by defining the percentage of scores in the related frequency distribution that are equal or lower value. In this study, the classification standards of 2%, 5%, 10%, 20%, and 30% were considered reasonable, thus enabling the categorization of SDSI into five classification corresponding to different compound event levels (Table 4).

Based on previous studies (Hao et al., 2019b; Zhou and Liu, 2018), the second indicator is a percentile-based approach to establishing threshold levels for hydrological drought and saltwater intrusion. Specifically, the 30% and 70% quantiles of runoff and salinity were employed to identify a sufficient number of compound events to validate the reliability of the proposed SDSI. Therefore, for the specific thresholds r_0 and s_0 of runoff and salinity, respectively, the occurrence of a compound drought and saltwater intrusion event Z can be expressed as:

Table 3
Goodness-of-fit of five candidate Copula functions.

Estuary	Criterion	Clayton	Frank	Gaussian	Gumbel	Joe
Little Back	AIC	−330.16	**−391.27**	−372.67	−372.32	−325.49
	BIC	−326.65	**−387.76**	−369.16	−368.81	−321.98
	LOGLIK	166.08	**196.64**	187.33	187.16	163.74
Ebro	AIC	**−56.69**	−51.51	−48.07	−56.09	−54.76
	BIC	**−53.08**	−47.90	−44.47	−52.49	−51.16
	LOGLIK	**29.34**	26.75	25.04	29.05	28.38
Rhine	AIC	−54.72	−46.70	−59.58	**−60.20**	−52.87
	BIC	−50.85	−42.83	−55.71	**−56.33**	−49.00
	LOGLIK	28.36	24.35	30.79	**31.10**	27.44
Orange	AIC	−162.06	**−204.22**	−202.72	−185.84	−149.85
	BIC	−158.18	**−200.34**	−198.83	−181.95	−145.97
	LOGLIK	82.03	**103.11**	102.36	93.92	75.93
Pearl River	AIC	−27.76	**−34.13**	−29.16	−28.61	−24.94
	BIC	−25.08	**−31.45**	−26.48	−25.93	−22.25
	LOGLIK	14.88	**18.06**	15.58	15.31	13.47
Murray	AIC	−62.78	−63.96	**−65.72**	−60.49	−52.54
	BIC	−58.89	−60.07	**−61.84**	−56.60	−48.65
	LOGLIK	32.39	32.98	**33.86**	31.24	27.27

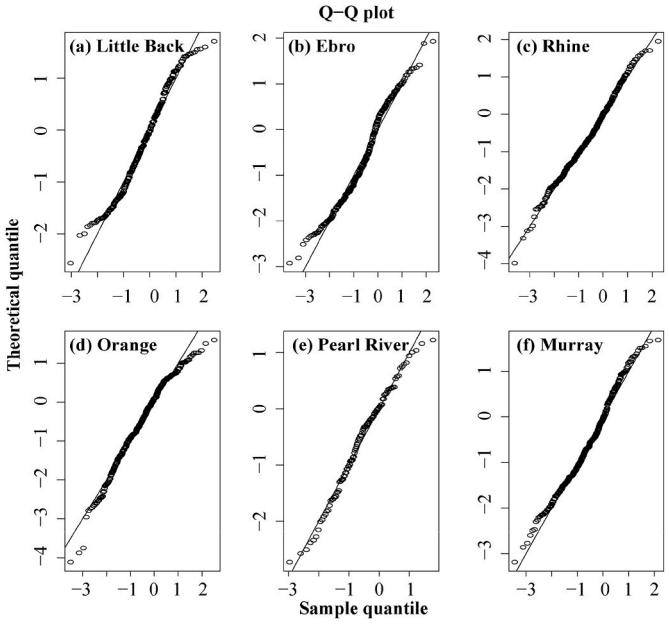

Fig. 3. Q-Q plot of SDSI at different estuaries.

Table 4
Categories of drought and saltwater intrusion conditions based on the SRI, SSI and SDSI.

Category	Compound drought-saltwater intrusion condition	Percentile change	SRI/SSI/ SDSI
Grade 0	Abnormal	(20, 30]	(-0.8, −0.5]
Grade 1	Moderate	(10, 20]	(-1.3, −0.8]
Grade 2	Severe	(5, 10]	(-1.6, −1.3]
Grade 3	Extreme	(2, 5]	(-2, −1.6]
Grade 4	Exceptional	≤2	≤-2

$$z = \begin{cases} 1, \mathrm{R} \le r_0, \mathrm{S} > s_0 \\ 0, otherwise \end{cases} \tag{6}$$

This indicator can be determined through the concurrence of drought and saltwater intrusion over a specific period. A value of Z = 1 indicates the presence of a compound drought-saltwater intrusion event, while a value of Z = 0 suggests the absence of such an event.

Following Zscheischler and Seneviratne (2017), the third indicator in this study utilizes PMF method to assess the likelihood of CDSEs. Similar to the percentile-based thresholds method, drought and saltwater intrusion events were defined using the 30th and 70th percentiles, respectively, and the independent joint probability was 0.09. The PMF can be express as:

$$\begin{aligned} \mathrm{PMF} &= \frac{f(\text{Compound drought and saltwater intrusion event})}{f(\text{drought}) * f(\text{saltwater intrusion})} \\ &= \frac{\text{Compound drought and saltwater intrusion event frequency (\%)}}{9\%} \end{aligned} \tag{7}$$

3.3. The modified Mann-Kendall (MMK) trend test method and relative importance analysis

The traditional Mann-Kendall (MK) trend test, as a nonparametric statistical test, is extensively used to detect the trend characteristics of hydro-climatology series (Wu et al., 2020). The MK method is based upon the assumption that time series are independent and random. Nevertheless, it is noteworthy that time series tend to have autocorrelation, which affects the significance of the test results (Huang et al., 2016). To address this issue, the MMK trend test method has been developed to effectively eliminate the autocorrelation component of time series and thereby to enhance the test capability of the MK method. Consequently, the MMK method is employed in this paper to identify the temporal trend characteristics of SDSI in the estuary. The calculation process is as follows:

Firstly, statistic S is calculated as follows:

$$S = \sum_{i<j} \mathrm{sgn}(x_j - x_i) \tag{8}$$

where

$$\mathrm{sgn}(x_j - x_i) = \begin{cases} 1, x_j > x_i \\ 0, x_j = x_i \\ -1, x_j < x_i \end{cases} \tag{9}$$

Secondly, the variance of S is computed:

$$Var(S) = \frac{n(n-1)(2n+5)}{18} \tag{10}$$

thirdly, the modified variance of S is estimated.

$$V*(S) = Var(S) * Cor \tag{11}$$

where *Cor* refers to the autocorrelation correction, which can be

estimated as follows:

$$Cor = 1+\frac{2}{n(n-1)(n-2)}\sum_{k=1}^{n-1}(n-1)(n-k-1)(n-k-2)r_k \quad (12)$$

where

$$r_k = \frac{\sum_{i=1}^{n-k}(x_i - m)(x_{i+k} - m)}{\sum_{i=1}^{n}(x_i - m)^2} \quad (13)$$

Finally, the standardized statistic Z is calculated.

$$Z = \begin{cases} \frac{S-1}{\sqrt{V*(S)}}, S > 0 \\ 0, S = 0 \\ \frac{S+1}{\sqrt{V*(S)}}, S < 0 \end{cases} \quad (14)$$

Changes in the severity of CDSEs may be attributed to changes in runoff and salinity. In light of the previous studies (Kang et al., 2022; Wu et al., 2020, 2021), this study used a stepwise multiple regression model to assess the relative importance of runoff and salinity on severity trends, which was calculated by the R package "claimpo".

4. Results

4.1. Performance of SDSI

The PMF of CDSEs in various estuaries, revealing a consistently high value of the PMF has been observed in all estuaries (Table 5). To be specific, the Little Back, Orange and Pearl River estuaries exhibit higher PMF values, suggesting a greater frequency of compound events in the three estuaries. Due to space limitations, the Pearl River and Little Back estuaries were used as examples to represent river-dominated estuary and tide-dominated estuary, respectively, in order to illustrate the properties of SDSI. The SRI, SSI, and SDSI values in the Pearl River and Little Back estuaries were compared to better visualization (Fig. 4). Low and negative SRI and SSI value indicates severe drought condition and saltwater intrusion, respectively. Similarly, a low and negative SDSI value indicates compound drought and saltwater intrusion conditions. The variation trend of SDSI value was relatively consistent with those of SRI and SSI values, and the increase or decrease in SRI and SSI values cause SDSI values to increases or decreases accordingly, demonstrating the basic properties of SDSI under drought and saltwater intrusion. Similar results regarding the comparison of these three indices were observed among other estuaries (Figure S1).

The black rectangular boxes depict the occurrences of CDSEs in Pearl River in January 2005 and in Little Back Estuary in June 2002 and November 2012, with corresponding SDSI values of −1.58, −1.86 and −2.57, respectively (Fig. 4(a) and (c)). These values reflect the severity of extreme drought and saltwater intrusion conditions during these CDSEs. The percentile-based thresholds method, which identifies the occurrence of compound drought events, aligns with the low and negative SDSI values (Fig. 4(b) and (d)). While the percentile-based thresholds method can identify the occurrence of compound drought events using different thresholds, it fails to evaluate their severity level, which can be visually represented by the proposed SDSI. Furthermore, the green rectangular box illustrates that neither SRI nor SSI was able to detect the occurrence of drought (saltwater intrusion) with a threshold of −1 (Fig. 4(a)). However, the compound index (SDSI) effectively captured the occurrence of CDSEs, proving its capability to combine information on both runoff and saltwater intrusion and to detect CDSEs sensitively and accurately. Meanwhile, SDSI was generally lower than SRI and SSI, illustrating that the revealed wetness of SDSI is lower than that of SRI, while the drought status of SDSI was higher than that of SRI, which reflects the severity of SDSI for hydrological drought events exacerbated by saltwater intrusion (Fig. 4(a) and (c)).

Additionally, SDSI captures the characteristics of both hydrological drought and saltwater intrusion as it is derived from runoff and salinity. The correlation analysis among the three indices reveals a correlation coefficient of 0.50 between SRI and SSI for Pearl River. Furthermore, a higher correlation coefficient of 0.82 and 0.87 is observed between the composite index (SDSI) and the univariate indices of SRI and SSI, respectively (Fig. 5). For Little Back Estuary, the correlation coefficient between SRI and SSI was 0.88, while those between the SDSI and the univariate indices (SRI and SSI) were 0.96 and 0.93, respectively. It is noteworthy that the correlation between the two univariate indices was obviously lower than that between the SDSI and the univariate indices. This suggests that to some extent, SRI may be limited in its ability to accurately reflect the occurrence of saltwater intrusion, while SSI may not be an optimal tool for assessing hydrological drought. In contrast, the constructed composite index (SDSI) is relatively better able to reflect the properties of CDSEs, with further evidence for the high sensitivity of the SDSI in detecting CDSEs. Similarly, detailed correlation analyses were also conducted for the indices of the other estuaries (Figure S2).

To further demonstrate the properties of the SDSI, scatter plots of SRI and SSI were presented in the Little Back Estuary (Fig. 6), where the size of the scatter corresponds to the absolute value of SDSI. For instance, the dots representing the 2002 and 2012 CDSEs in the third quadrant, correspond to the low and negative SRI and SSI values, indicating that the SDSI values are smaller when the probability $P(X \leq x \wedge Y > y)$ is lower. In addition, an interesting characteristic of SDSI is that there are several dots in the second quadrant where CDSEs occur. This indicates that although individual events may not be extremes conditions, the combination of events can still lead to compound drought and saltwater intrusion conditions, which is consistent with the depiction of the green rectangular box (Fig. 4(a)). Furthermore, few dots fell into the fourth quadrant, which suggests that the probability of saltwater intrusion without drought is low. As a result, the SDSI provides a valuable tool for evaluating the severity of CDSEs. Similar results about the scatter plot between SRI and SSI can also be observed for the other estuaries (Figure S3).

4.2. Temporal variation of CDSEs in estuaries

The trend characteristic of the severity of CDSEs in each estuary was analyzed using the MMK trend test method on the entire time series of SDSI and monthly SDSI (Fig. 7). A positive *Zs* value indicates a decreasing trend in the severity of CDSEs, while a negative *Zs* value indicates an increasing trend in CDSEs. The results showed that a continuous decreasing trend was observed in the timeseries of Little Back, Ebro and Orange estuaries with *Zs* value of −2.43, −3.63 and −3.23, respectively. Notably, the *Zs* value for Little Back, Ebro, and Orange passed the significance test at the 0.01 level, indicating that a significant increase in CDSEs during the study period. The increasing trend in CDSEs (decreasing trend in SDSI) and declining trend in SSI are in accordance with the increasing trend in salinity in the Orange Estuary as reported by Thorslund et al. (2021) (Figure S4(b)). The SDSI for the Rhine Estuary demonstrated an increasing trend for all months, and the overall trend for SDSI witnessed a significant increasing trend with a *Zs* value of 3.75. The Murray Estuary showed an increasing trend except for July through November, which exhibited a decreasing trend, indicating CDSEs were alleviated. This is in consistence with the results of Thorslund et al. (2021), which suggest that salinity in the Murray Estuary decreased predominantly (Figure S4(b)). As for the Pearl River Estuary,

Table 5
The likelihood of compound drought and saltwater intrusion events (bold letter indicates high value of PMF).

Estuary	Little Back	Ebro	Rhine	Orange	Pearl River	Murray
PMF	**2.83**	1.39	1.40	**2.10**	**2.06**	1.60

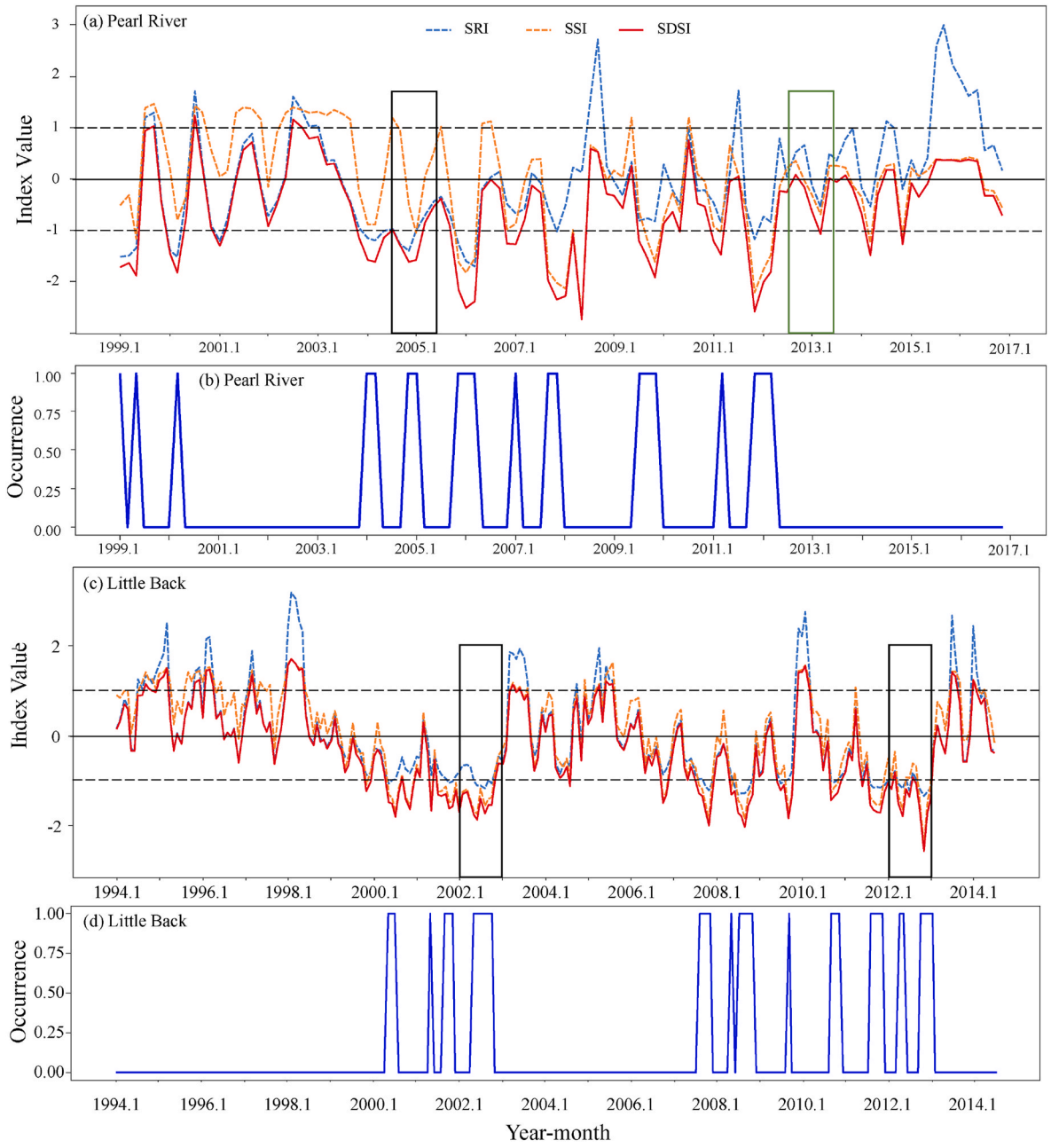

Fig. 4. Series of three indices (SRI, SSI and SDSI) and occurrence of compound events (1 for occurrence and 0 for nonoccurrence) at Pearl River (a, b) and Little Back (c, d) estuaries.

the SDSI exhibited a decreasing trend in October and November, and an increasing trend in January, February and March. The insignificant increase in entire timeseries of SDSI suggests that the compound drought and saltwater intrusion in the Pearl River during the dry season has been alleviated to a certain degree, possibly due to more precipitation and corresponding increase in runoff during the dry season in 2013–2016. This is in line with the results reported by Huang and Wang (2021), which showed significant drought relief after 2013.

Trends in SRI and SSI may be related to changes in the severity of CDSEs. In this study, the trends of the SRI and SSI over the study period were also evaluated using MMK (Figure S4(a) and (b)). Notably, a significant decreasing trend of SSI value less than −1.68 was observed in the estuaries of Little Back, Ebro, Rhine, Orange, and Murray (Figure S4 (a)). Previous studies have shown a downward trend of runoff in these estuaries (Leblanc et al., 2012; Shi et al., 2019; Thorslund et al., 2021; Vicente-Serrano et al., 2017). The SSI values for the Little Back, Ebro, Orange, and Pearl River estuaries increased, which is consistent with previous studies that suggest a decreasing trend in salinity within these estuaries (Figure S4(b)) (Liu et al., 2018, 2019; Merchán et al., 2018; Romaní et al., 2010; Thorslund et al., 2021). By contrast, an upward tendency was observed in the salinity of Murray and Rhine estuaries, which is in line with the increasing trend in salinity in previous studies (Thorslund et al., 2021; Verbrugge et al., 2012). Verbrugge et al. (2012) found a drastic decline in salinity since 1986, owing to the implementation of effective water pollution control measures (i.e., international treaties aimed at reducing salinity loads of the Rhine). According to Loch and Gregg (2018), a crucial intervention for mitigating the salinity of the Murray River involves implementing salt interception schemes in high-risk areas. Since the implementation of these interventions in 1989, the salinity levels in the river have consistently remained below the threshold of 800 μS/cm. The increased severity of compound extremes caused by reduced runoff and increased salinity

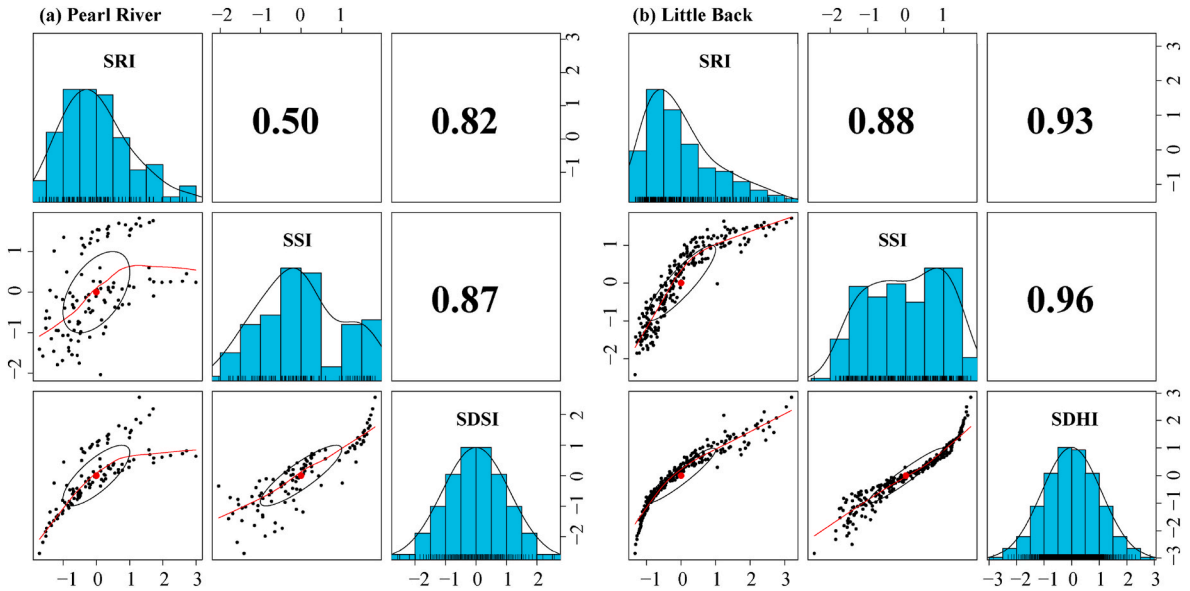

Fig. 5. Correlation analysis between indices at Pearl River (a) and Little Back (b) estuaries.

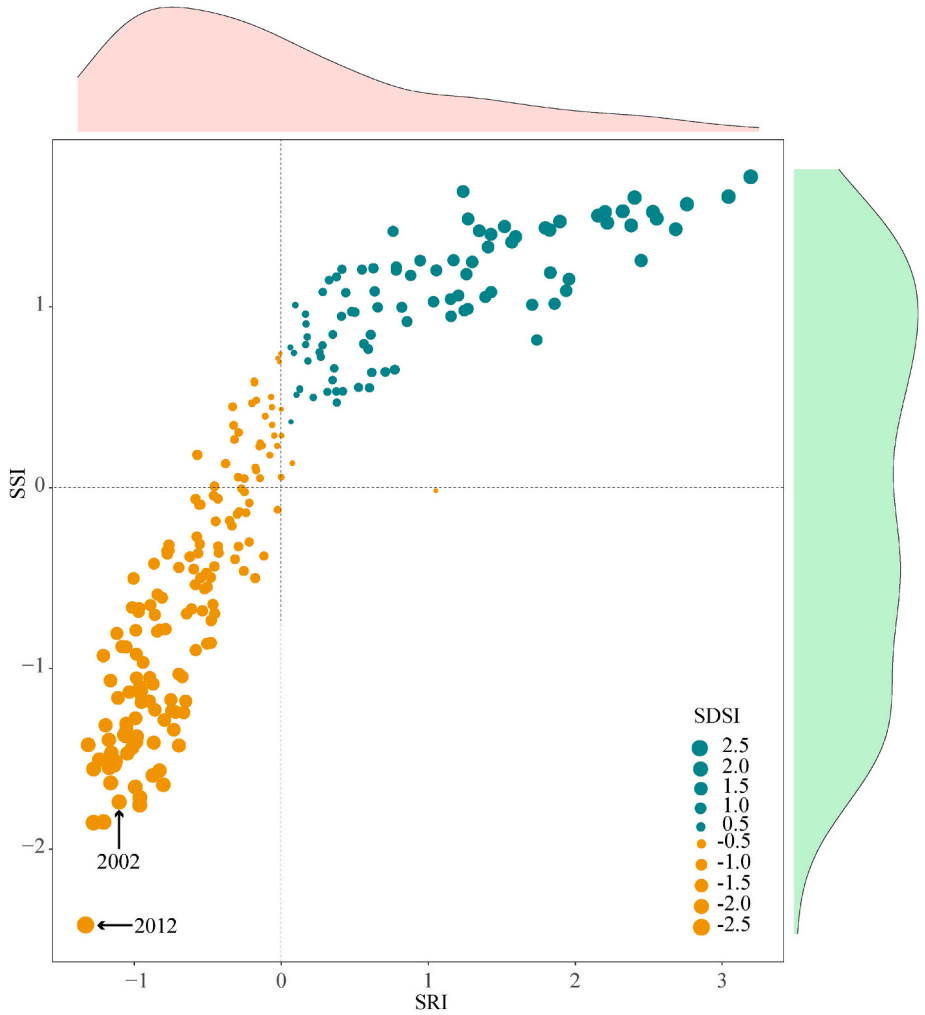

Fig. 6. Scatter plot between SRI and SSI at Little Back Estuary (the size of the scatter plot is determined by SDSI, and yellow and green indicate negative values and positive values, respectively). (For interpretation of the references to colour in this figure legend, the reader is referred to the Web version of this article.)

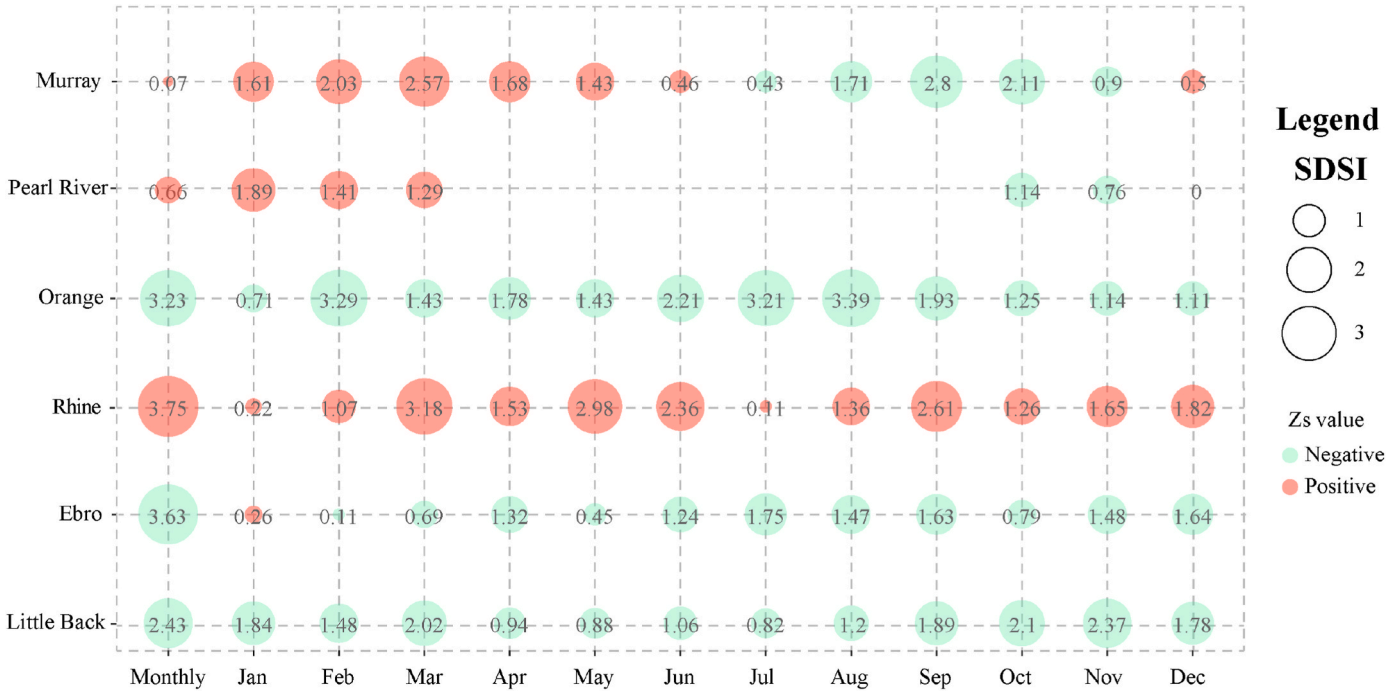

Fig. 7. The trend of SDSI at different estuaries.

may pose significant challenges to the social and ecological systems of these estuaries.

4.3. Spatial analysis of CDSEs in estuaries

Analysis of CDSEs helps to better understand their condition in estuaries against the backdrop of decreased upstream runoff and global sea level rise. During the study period, the number of CDSEs varied within the six estuaries (Fig. 8). Specifically, the Little Back, Ebro, Rhine, Orange, Pearl River, and Murray estuaries recorded 108, 166, 217, 176, 52 and 215 CDSEs, respectively, corresponding to a frequency of compound occurrence of 43.72%, 61.25%, 60.96%, 48.89%, 48.15% and 59.72%, respectively. In particular, the probability of CDSEs occurring in the Ebro, Rhine and Murray estuaries was the highest at nearly 60%. To better understand the characteristics of the CDSEs, this study compared the frequency of droughts based on the constructed SDSI and on other univariate indices (SRI and SSI). Five different thresholds (−0.5, −0.8, −1.3, −1.6, and −2) were used to classify the severity of CDSEs into abnormal, moderate, severe, extreme, and exceptional categories. The number of occurrences of CDSEs was extracted for each threshold, and the frequency of occurrences of CDSEs at different levels was obtained by dividing the number of occurrences by the total number of the months in the study period. Overall, the proportion of CDSEs varies at different thresholds (Fig. 8). The moderate CDSEs occurred most frequently in each estuary, with a frequency ranging between 15 and 20%. Notably, the frequency of CDSEs in the Rhine Estuary was the highest among all estuaries, with a value of 20.51%. Besides, it is noteworthy that exceptional CDSEs may occur even when hydrological droughts do not fall into the exceptional categories (as can be observed in the Little Back, Ebro and Pearl River estuaries). This observation is consistent with the above finding where individual events that do not meet the criteria for extreme conditions may lead to extreme impacts when occurring simultaneously. Moreover, as the severity level of CDSEs increases (i.e., the threshold value decreases), the frequency of SDSI becomes more prominent for all estuaries when compared to univariate indices (SRI and SSI). Overall, compared to univariate indices (SRI and SSI), the use of SDSI resulted in a higher frequency of severe CDSEs (including severe, extreme, and exceptional levels). This can also be attributed to interaction between drought and saltwater intrusion. Prolonged drought could induce saltwater intrusion, while saltwater intrusion, in turn, exacerbates drought conditions. Consequently, these interactions contribute to the occurrence of more severe compound drought and saltwater intrusion events, significantly impacting freshwater availability within the estuary.

The SDSI was also used to obtain the characteristics of CDSEs, including duration and severity, for each estuary. The variation in CDSE characteristics within each estuary is shown in violin plot (Fig. 9), with substantial differences observed in the characteristics of CDSEs across different estuaries. Specifically, the average durations of CDSEs in the Little Back, Ebro, Rhine, Orange, Pearl River and Murray estuaries were 5.14, 6.38, 4.42, 5.50, 3.06 and 7.68 months, respectively (Fig. 9(a)). Similar spatial patterns were observed between CDSEs severity and duration, with corresponding mean CDSEs severity values of 3.48, 5.66, 3.60, 4.54, 2.68 and 5.94, respectively (Fig. 9(b)). Specifically, the Murray Estuary had the highest mean severity and longest mean duration of CDSEs among the six estuaries, and the interquartile range was larger than that in other estuarine areas, indicating that the Murray Estuary experienced a highly variable CDSEs conditions. The kernel density distributions of the Little Back, Ebro, and Rhine estuaries had a relatively consistent patterns, indicating that these estuaries experienced severe and long-lasting CDSEs. Notably, the median duration and severity of CDSEs in the Orange Estuary were relatively small, at 2 months and 0.88, respectively, suggesting that this estuary is primarily subject to short-duration and low-severity CDSEs. However, the presence of several outliers in the violin plot suggests the occurrence of extreme CDSEs in the Orange Estuary. CDSEs were observed in the Orange Estuary from January 2003 to January 2006 (Figure S1(c)), with duration and severity of 37 months and 40.55, respectively (Fig. 9), which is generally in line with previous studies (Hao et al., 2019a; Masih et al., 2014). Compared to the other estuaries, the non-existence of CDSE outliers in the Pearl River Estuary can be attributed to the fact that only CDSEs in the dry season were considered. On top of that, the characteristics (duration and severity) of the univariate indices (SRI and SSI) (Figure S5) were also compared to those of the composite index (SDSI), and the latter showed more severe duration and severity. These quantitative results imply that the characteristics of CDSEs pose a higher risk

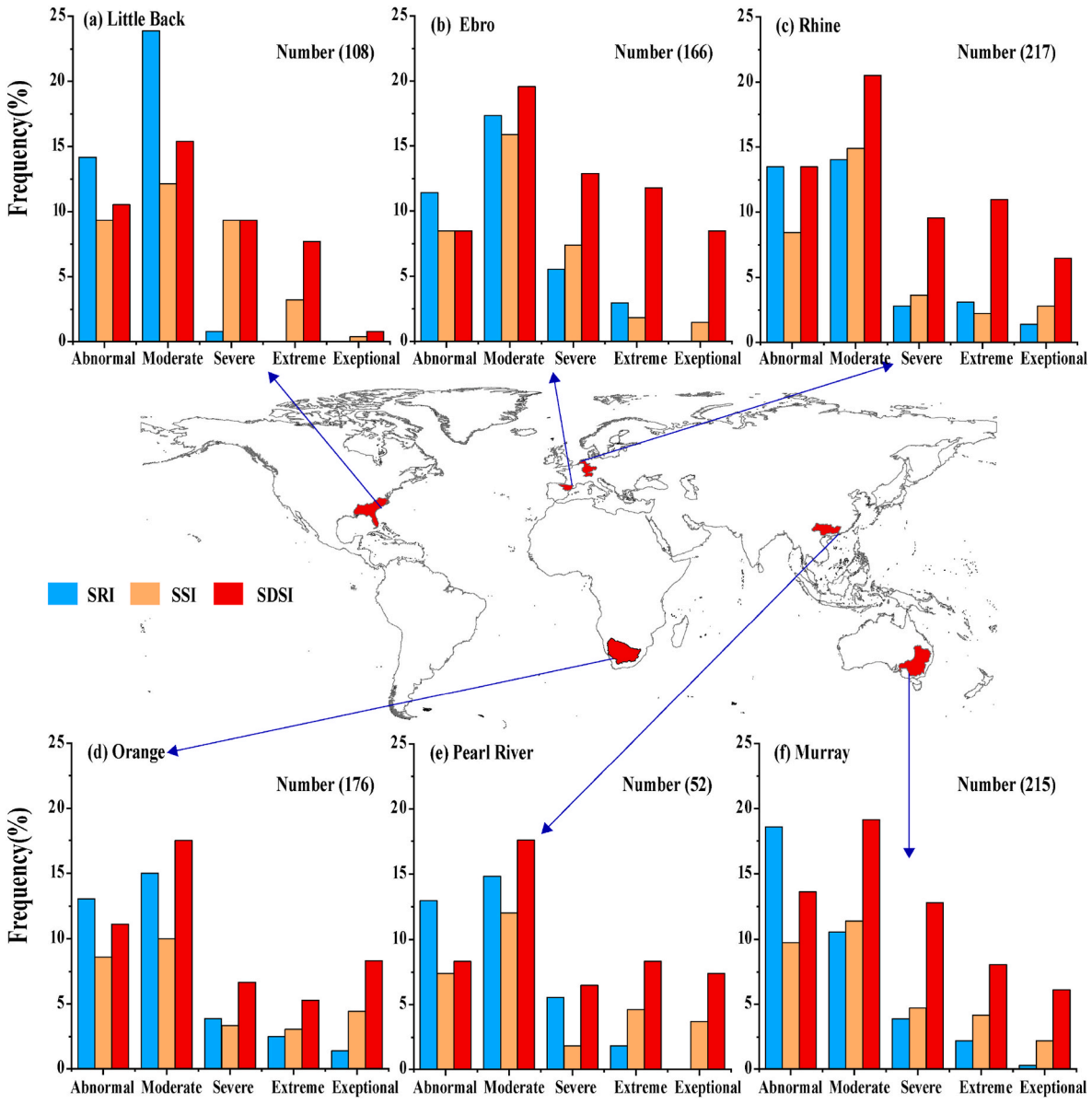

Fig. 8. Frequency of compound events at different thresholds at different estuaries. The number in parentheses refer to the number of compound drought and saltwater intrusion events.

than those of individual events.

4.4. Relative contribution of change in runoff and saltwater intrusion to the SDSI

In the context of sea level rise, extensive human- and climate-driven changes are observed in most estuaries, contributing to a declining trend in estuarine runoff and thus rendering estuaries more vulnerable to droughts. When hydrological drought coincide with saltwater intrusion, a hazard of concurrent drought and saltwater intrusion form in estuaries, adversely affecting the social and ecological environment of the area. This study classifies estuaries into two types: river-dominated and tide-dominated estuaries (Table 1). Specifically, river-dominated estuaries are usually located near the mouth of the river with sandbars being physical barriers, characterized by highly variable salinity regimes, hydrologic conditions (Bourman et al., 2022; Cooper, 2002; Kärnä et al., 2015; Lu et al., 2022; Phlips et al., 2023; Wei et al., 2022). During the dry season, nonetheless, the freshwater runoff of the river decreases, causing a gradual increase in salinity. Tide-dominated estuaries, in contrast, are typically located within the mouth of river and form a tidal zone. The water level in these estuaries is heavily influenced by tidal fluctuations, causing them to vary with the rise and fall of the tides (Azhikodan et al., 2021; Bittar et al., 2016; Chen and Zhang, 2020; Codden et al., 2022; Desjardins et al., 2012; Hoitink and Jay, 2016; Hu et al., 2018; Nienhuis et al., 2020; Qiu et al., 2022; Rijnsburger et al., 2021). During the drought or low-rainfall period, the decrease in river runoff, combined with tidal movements, can make saltwater intrusion worse and lead to further increases in salinity levels within the estuary. Thus, both river-dominated and tide-dominated estuaries induce saltwater intrusion due to reduced river runoff (Liu et al., 2019; Peters et al., 2022; Wang et al., 2022a,b,d).

The severity of changes in the compound drought and saltwater intrusion may be influenced by the individual or combined effects of variations of runoff and saltwater intrusion. In the case of greater saltwater intrusion, the severity of CDSEs is expected to increase under conditions of constant runoff. To further investigate the relative contribution of runoff and saltwater intrusion to the severity of river-dominated and tide-dominated CDSEs, this study employed stepwise

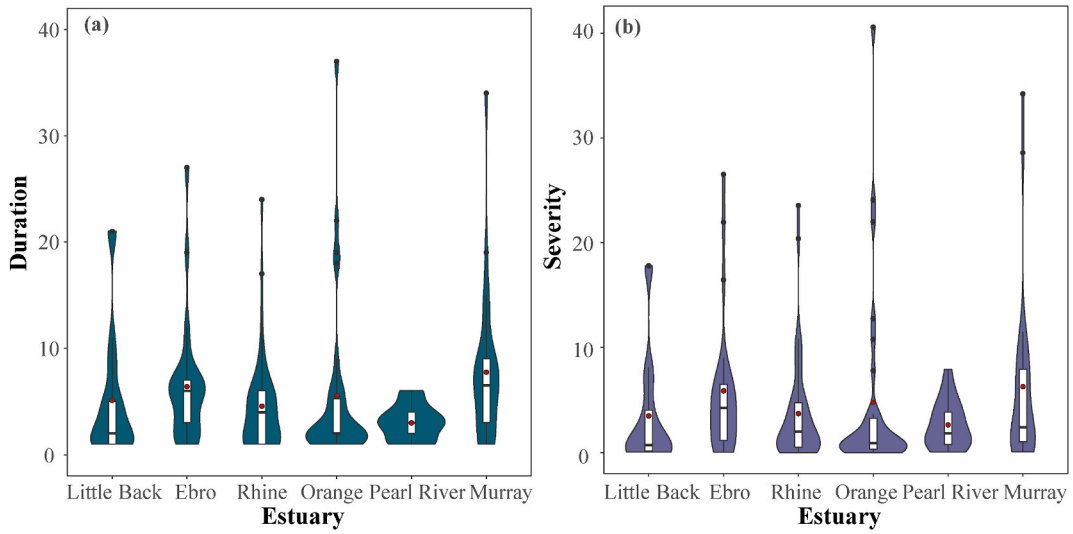

Fig. 9. The characteristics of compound events at different estuaries.

multiple regression model to assess the individual effect of these variables on the SDSI. Four models (First, LMG, CAR, and Last) were selected for contribution analysis in this study (Table 6). Generally, the relative contributions of runoff and saltwater intrusion to the trends of variation of SDSI are consistent in four models demonstrating the robustness of the results. In all estuaries except for Murray, the contribution of saltwater intrusion to the change in SDSI was greater than that of runoff (the relative contribution of saltwater intrusion exceeds 54%), indicating that the effect of saltwater intrusion likely dominates the change in SDSI in estuaries. Specifically, saltwater intrusion was the largest contributor to the SDSI variation in Orange Estuary, with a range of 81.54%–95.30%, much larger than that of runoff. As for the Murray Estuary, the relative contribution of hydrological drought and saltwater intrusion to the SDSI were comparable. These results suggest that saltwater intrusion is likely to dominate the severity of change in SDSI in the estuaries. In addition, there is little difference in the relative contribution of SDSI between tide-dominated and river-dominated estuaries.

5. Discussion

5.1. Sensitivity of marginal distributions, copulas and thresholds

Copulas are statistical measures that are able to connect any two or more relevant variables from arbitrary marginal distributions to flexibly yield their joint distributions (Alizadeh et al., 2020). The fewer constraints and ease of use in joining the marginals together have led to the widespread application of copulas in drought assessment and ecological researches (Fang et al., 2019). In this study, the SDSI was calculated by utilizing the optimal distribution function to fit the marginal distribution and the optimal copula to combine runoff and salinity. Other candidate functions, such as the Weibull distribution for runoff, the log-normal and gamma distributions for salinity, and Gaussian and Gumbel function for the joint copula, showed comparable performance for the Little Back Estuary (Tables 3 and 4). This kindled an interest in investigating the sensitivity of various marginal distributions when using SRI and SSI to assess hydrological drought and saltwater intrusion, as well as the sensitivity of different copulas when using SDSI to assess CDSEs. Therefore, candidate distribution functions were utilized to calculate SRI and SSI, while other copula functions were employed to combine runoff and salinity to evaluate sensitivity in this study. A comparative analysis was conducted on the SRI, SSI, and SDSI curves generated using different distributions and copula functions (Fig. 10, Figure S6, and Figure S7). It can be observed that these time series (SRI, SSI and SDSI) are highly consistent with each other, while differing slightly in the assessment of extreme value conditions, which generally aligns with the research results of Liu et al. (2016). Previous studies have also indicated the importance of selecting optimal distribution functions for hydrological drought assessment, as well as the significance of selecting optimal copula functions for multivariate joint indices (Chang et al., 2016; Chen et al., 2018; Huang et al., 2016; Liu et al., 2016; Wang et al., 2020a, 2020b).

Furthermore, this study analyzed the characteristics of CDSEs for each estuary based on five thresholds (−0.5, −0.8, −1.3, −1.6, and −2) for comparison (Fig. 9, S8, and S9). According to these five threshold levels, as the thresholds became extreme, the frequency of occurrence decreased, the duration shortened, and the severity lessened, which is generally consistent with previous studies (Guo et al., 2019; Hao et al., 2019b). CDSEs based on a threshold of −2.0 indicate the most severe condition, and two compound drought-salinity events were identified in Little Back Estuary, with an average duration of 2 months and an average severity of 0.3. However, using a threshold of −0.5 was sufficient to capturing enough CDSEs for statistical analysis, yielding reliable results. The selection of different distributions, copulas, and thresholds has a considerable impact on estimating the frequency, severity, and

Table 6
Relative importance of runoff and salinity for the SDSI in different estuaries.

Estuary	First		LMG		CAR		Last	
	Runoff	Salinity	Runoff	Salinity	Runoff	Salinity	Runoff	Salinity
Little Back	44.13	55.87	40.45	59.55	37.48	62.52	24.46	75.54
Ebro	44.68	55.32	42.68	57.32	42.08	57.92	38.25	61.75
Rhine	45.82	54.18	44.31	55.69	43.89	56.11	41.09	58.91
Orange	18.46	81.54	12.81	87.19	11.22	88.78	4.70	95.30
Pearl River	45.96	54.04	44.63	55.37	44.31	55.69	42.02	57.98
Murray	50.03	49.97	50.05	49.95	50.05	49.95	50.08	49.92

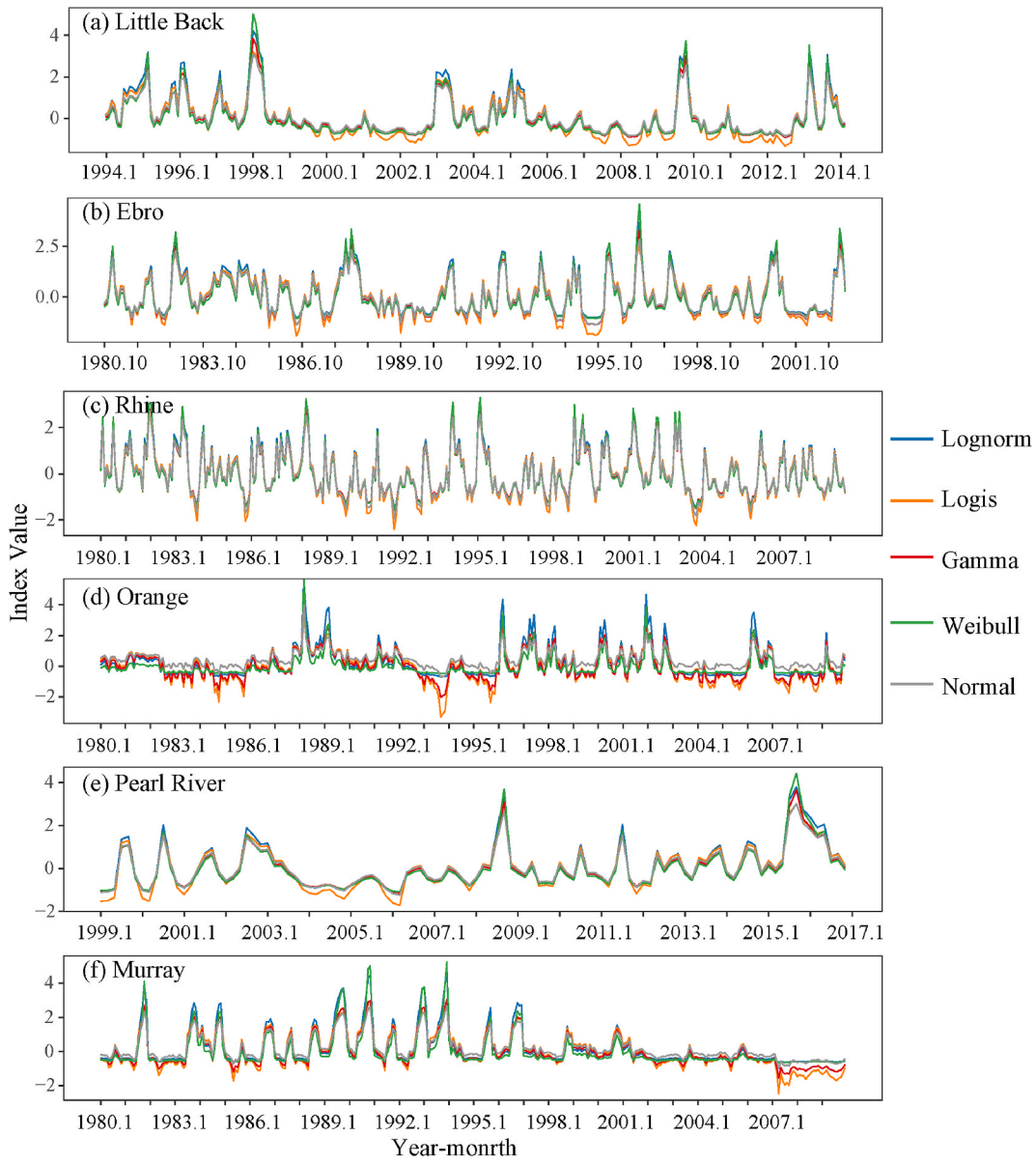

Fig. 10. Comparison analysis of the monthly SRI time series calculated from different distributions for each estuary.

duration of extreme events. Exploring these sensitivities offers a more comprehensive understanding of the characteristics of CDSEs, revealing how these events can be characterized differently based on varying assumptions and parameter configurations. Therefore, it can be seen that different distributions, copulas and thresholds are extremely important for evaluating the extreme conditions of CDSEs.

5.2. *The merits and limitations of SDSI*

Concurrent extreme events have more serious environmental and social impacts than individual extreme events (Feng et al., 2023; Zhang et al., 2021). Previous studies on compound events are focused on the concurrence of droughts and heatwaves in recent years (Hao et al., 2020; Li et al., 2021a,b; Wu et al., 2019a, 2021; Yu and Zhai, 2020). However, further investigation is desperately needed on other concurrent extremes, such as concurrent hydrological droughts and saltwater intrusion, as these events can be significantly more severe than individual extreme events. For univariate indices, runoff is commonly regarded as a primary factor in the occurrence and assessment of hydrological droughts (Wang et al., 2021a; Wu et al., 2022; Zhang et al., 2018; Zhou et al., 2021). Over the past few decades, due to global warming, hydrological droughts in estuaries have also been influenced by a variety of factors, including precipitation, runoff, topography, tide level, salinity, wind speed, etc (He et al., 2018). Therefore, relying solely on runoff-based SRI may exert limitations on fully monitoring drought conditions in the estuaries. Moreover, a number of studies have demonstrated a strong relationship between estuarine drought and saltwater intrusion (Conrads and Darby, 2017; He et al., 2018; Jones and van Vliet, 2018; Wei et al., 2022). Specifically, during the periods of high flow, the intrusion of saltwater upstream is hindered, whereas during the drought periods driven by tidal forces, saltwater intrusion moves upstream, causing a significant rise in the salinity level of the river (Conrads and Darby, 2017; Jones and van Vliet, 2018). The concurrence of hydrological drought and saltwater intrusion in estuaries can amplify the impacts of these individual extremes, resulting in severe consequences for local ecosystems and societies. However, the current hydrological drought indices rarely take into account the characteristics of saltwater intrusion. This paper addresses this gap by constructing a new index that accounts for both hydrological drought and saltwater intrusion, and demonstrates its effectiveness in identifying and

evaluating compound drought and saltwater intrusion in estuaries.

Firstly, the SDSI utilized in this study can serve as an early warning system for CDSEs in estuaries, and more accurately reflect the severity of these events. It is worth noting that the percentile-base threshold method was employed to extract the occurrence of CDSEs in estuaries to enhance the robustness of the SDSI. SDSI effectively captured the occurrence of CDSEs (Fig. 4(a) and (c)), which were identified using the percentile-based threshold method (Fig. 4(b) and (d)). Furthermore, SDSI provids insight into the severity of these events. Both methods offer distinct advantages. The percentile-based threshold method is simpler and easier to calculate, while SDSI is able to distinguish the characteristics and severity level of multiple compound events. Previous studies found that the negative effects of compound events are not solely determined by their frequency and duration, but also by the grades of their severity (Li et al., 2021a,b; Wang et al., 2021b; Wu et al., 2020). Therefore, compared to the percentile-based threshold method, SDSI proved to be a practical tool for identifying CDSEs.

Secondly, compared to the traditionally used SRI, SDSI is capable of monitoring CDSEs better and shows good consistency with historical records. As illustrated by the green rectangular box (Fig. 4), the proposed SDSI exhibits greater sensitivity than SRI and can effectively capture information on CDSEs, thus overcoming one of the limitations of the SRI that only considers runoff. As a standardized index, SDSI represents dimensionless characteristics, thereby enabling the comparison of compound events in time and space (Mishra and Singh, 2010; Wu et al., 2022). For each estuary, the trend of SDSI is generally consistent with that of the drought index (SRI), but SDSI exhibits higher severity levels in most cases. To be specific, the wetness state revealed by SDSI was lower than that of SRI (SRI with high value), while its drought state was higher than that of SRI (SDSI with low value). The principal reason is that the SDSI incorporates both runoff and salinity, which results in a reduction in water quantity during hydrological droughts in estuaries. Additionally, saltwater intrusion exacerbates water scarcity in terms of water quality, leading to more severe compound extreme conditions that further reduce the water availability in estuaries. The contribution analysis based on multiple linear regression further suggests that saltwater intrusion may be the main contributor to the increased severity of compound drought and saltwater intrusion in estuaries. Meanwhile, this study addresses, to a certain degree, the gap in current quantitative research into water scarcity that neglects water quality (Jones and van Vliet, 2018).

Finally, it should be noted that the proposed index has certain limitations. CDSEs are influenced by various factors, including precipitation, runoff, topography, tide level, salinity, and wind speed (He et al., 2018). However, this study only considered runoff and salinity in the description of CDSEs. Additionally, the discussion only covered five commonly used copulas. In future research, the index can be expanded to incorporate more variables and establish joint functions among multi-variables, and the application of high-dimensional copula will become a new research direction (Wang et al., 2020a). Besides, the proposed index is illustrated based on the gauged observations of estuaries in this study. It can be extended for CDSEs monitoring in different estuaries worldwide using different types of datasets, including model simulations, remote sensing products, and reanalysis products (Hao et al., 2020). Moreover, while this study primarily focuses on defining CDSEs at a monthly time scale, saltwater intrusion is typically characterized using daily time scale data (Zhou et al., 2020). Future research should aim to further develop SDSI as the core, and consider characterizing compound drought and saltwater intrusion conditions at finer time scales (e.g. days or weeks). This could enhance the assessment of the impact of CDSEs in estuaries.

6. Conclusion

Compared to individual extreme, the compound extreme events exert more profound impacts on both the environment and society. To date, little attention has been paid to the characteristics of CDSEs, especially with regards to the severity of concurrent extreme events. SDSI was developed in this study to quantify CDSEs in the estuary. The SDSI was further graded to compare the severity of CDSEs during the observation period. The conclusions are summarized as follows:

(1) Through the fitting of five different probability distributions, it was found that the optimal distribution functions of runoff in estuaries were all Lognorm, while those for salinity varied among different estuaries. Additionally, the copula-based SDSI effectively characterizes the hydrological drought features of estuaries by combining the characteristics of runoff and salinity.
(2) Compared to the traditional SRI, SDSI sensitively monitors CDSEs across all estuaries. Specifically, SDSI typically shows a higher severity compared to SRI, representing severe drought characteristics in the dry conditions, while indicating lighter wetness characteristics in wet conditions. The difference is attributed to the exacerbation of drought conditions caused by saltwater intrusion, resulting in a more severe water shortage in estuaries.
(3) The contributions of runoff and salinity to SDSI were quantified using four regression models, and the consistency of these four models indicates the robustness of the results. Specifically, drought induced saltwater intrusion, and salinity was relatively more important to the severity of change in SDSI than runoff in the estuaries.
(4) The severity of SDSI was graded according to different thresholds, illustrating that moderate CDSEs occurred most frequently among all estuarine events. Additionally, serious CDSEs (i.e. severe, extreme, and exceptional) were observed more frequently in the SDSI compared to the SRI.
(5) The duration of CDSEs varied among different estuaries, whilst similar spatial patterns were observed in the severity of CDSEs. Among all estuaries, the Murray Estuary experienced the most severe CDSEs, with an average duration of 7.68 months and a severity of 5.94.

CRediT authorship contribution statement

Dan Li: Methodology, Software, Validation, Investigation, Visualization, Writing – original draft. **Bingjun Liu:** Conceptualization, Funding acquisition, Project administration, Supervision. **Yang Lu:** Funding acquisition, Supervision, Validation, Writing – review & editing. **Jianyu Fu:** Supervision, Validation, Writing – review & editing.

Declaration of competing interest

The authors declare no conflict of interest.

Data availability

Data will be made available on request.

Acknowledgements

This study was supported by the National Natural Science Foundation of China (Grant Nos. 52179029, 51879289 and 52209047), Science and Technology Innovation Program from Water Resources of Guangdong Province (2023-01), the Innovation Fund of Guangzhou City water science and technology (GZSWKJ-2020-2), the Guangdong Basic and Applied Basic Research Foundation (2019B1515120052).

Appendix A. Supplementary data

Supplementary data to this article can be found online at https://doi.org/10.1016/j.jenvman.2023.119659.

References

Alizadeh, M.R., Adamowski, J., Nikoo, M.R., AghaKouchak, A., Dennison, P., Sadegh, M., 2020. A century of observations reveals increasing likelihood of continental-scale compound dry-hot extremes. Sci. Adv. 6 https://doi.org/10.1126/sciadv.aaz4571 eaaz4571.

Azhikodan, G., Hlaing, N.O., Yokoyama, K., Kodama, M., 2021. Spatio-temporal variability of the salinity intrusion, mixing, and estuarine turbidity maximum in a tide-dominated tropical monsoon estuary. Continent. Shelf Res. 225, 104477 https://doi.org/10.1016/j.csr.2021.104477.

Bittar, T.B., Berger, S.A., Birsa, L.M., Walters, T.L., Thompson, M.E., Spencer, R.G.M., Mann, E.L., Stubbins, A., Frischer, M.E., Brandes, J.A., 2016. Seasonal dynamics of dissolved, particulate and microbial components of a tidal saltmarsh-dominated estuary under contrasting levels of freshwater discharge. Estuar. Coast Shelf Sci. 182, 72–85. https://doi.org/10.1016/j.ecss.2016.08.046.

Bourman, R.P., Murray-Wallace, C.V., Wilson, C., Mosley, L., Tibby, J., Ryan, D.D., De Carli, E.D., Tulley, A., Belperio, A.P., Haynes, D., Roberts, A., Westell, C., Barnett, E. J., Dillenburg, S., Beheregaray, L.B., Hesp, P.A., 2022. Holocene freshwater history of the Lower River Murray and its terminal lakes, Alexandrina and Albert, South Australia, and its relevance to contemporary environmental management. Aust. J. Earth Sci. 69, 605–629. https://doi.org/10.1080/08120099.2022.2019115.

Brunner, M.I., Stahl, K., 2023. Temporal hydrological drought clustering varies with climate and land-surface processes. Environ. Res. Lett. 18, 034011 https://doi.org/10.1088/1748-9326/acb8ca.

Chang, J., Li, Y., Wang, Y., Yuan, M., 2016. Copula-based drought risk assessment combined with an integrated index in the Wei River Basin, China. J. Hydrol. 540, 824–834. https://doi.org/10.1016/j.jhydrol.2016.06.064.

Chen, J., Zhang, W., 2020. Impacts of tidal species on water level variations in Pearl River Delta channel networks. Regional Studies in Marine Science 35, 101110. https://doi.org/10.1016/j.rsma.2020.101110.

Chen, X., Li, F., Feng, P., 2018. Spatiotemporal variation of hydrological drought based on the optimal standardized streamflow index in luanhe river basin, China. Nat. Hazards 91, 155–178. https://doi.org/10.1007/s11069-017-3118-6.

Codden, C.J., Edwards, C.R., Stubbins, A., 2022. Non-conservative behavior of dissolved organic carbon in a Georgia salt marsh creek indicates summer outwelling. Estuarine. Coastal and Shelf Science 265, 107709. https://doi.org/10.1016/j.ecss.2021.107709.

Conrads, P.A., Darby, L.S., 2017. Development of a coastal drought index using salinity data. Bull. Am. Meteorol. Soc. 98, 753–766. https://doi.org/10.1175/BAMS-D-15-00171.1.

Cooper, J.A.G., 2002. The role of extreme floods in estuary-coastal behaviour: contrasts between river- and tide-dominated microtidal estuaries. Sedimentary Geology, Coastal Environment Change During Sea-Level Highstands 150, 123–137. https://doi.org/10.1016/S0037-0738(01)00271-8.

Cooper, J.A.G., 2001. Geomorphological variability among microtidal estuaries from the wave-dominated South African coast. Geomorphology 40, 99–122. https://doi.org/10.1016/S0169-555X(01)00039-3.

Desjardins, P.R., Buatois, L.A., Mángano, M.G., 2012. Chapter 18 - tidal flats and subtidal sand bodies. In: Knaust, D., Bromley, R.G. (Eds.), Developments in Sedimentology, Trace Fossils as Indicators of Sedimentary Environments. Elsevier, pp. 529–561. https://doi.org/10.1016/B978-0-444-53813-0.00018-6.

Fang, W., Huang, S., Huang, Q., Huang, G., Wang, H., Leng, G., Wang, L., Guo, Y., 2019. Probabilistic assessment of remote sensing-based terrestrial vegetation vulnerability to drought stress of the Loess Plateau in China. Remote Sensing of Environment 232, 111290. https://doi.org/10.1016/j.rse.2019.111290.

Feng, S., Hao, Z., Zhang, Y., Zhang, X., Hao, F., 2023. Amplified future risk of compound droughts and hot events from a hydrological perspective. J. Hydrol. 617, 129143 https://doi.org/10.1016/j.jhydrol.2023.129143.

Furlan, E., Pozza, P.D., Michetti, M., Torresan, S., Critto, A., Marcomini, A., 2021. Development of a multi-dimensional coastal vulnerability index: assessing vulnerability to inundation scenarios in the Italian coast. Sci. Total Environ. 772, 144650 https://doi.org/10.1016/j.scitotenv.2020.144650.

Genua-Olmedo, A., Alcaraz, C., Caiola, N., Ibáñez, C., 2016. Sea level rise impacts on rice production: the Ebro Delta as an example. Sci. Total Environ. 571, 1200–1210. https://doi.org/10.1016/j.scitotenv.2016.07.136.

Guo, Y., Huang, S., Huang, Q., Wang, H., Fang, W., Yang, Y., Wang, L., 2019. Assessing socioeconomic drought based on an improved multivariate standardized reliability and resilience index. J. Hydrol. 568, 904–918. https://doi.org/10.1016/j.jhydrol.2018.11.055.

Hao, Z., 2022. Compound events and associated impacts in China. iScience 25, 104689. https://doi.org/10.1016/j.isci.2022.104689.

Hao, Z., Hao, F., Singh, V.P., Ouyang, W., Zhang, X., Zhang, S., 2020. A joint extreme index for compound droughts and hot extremes. Theor. Appl. Climatol. 142, 321–328. https://doi.org/10.1007/s00704-020-03317-x.

Hao, Z., Hao, F., Singh, V.P., Zhang, X., 2019a. Statistical prediction of the severity of compound dry-hot events based on El Niño-Southern Oscillation. J. Hydrol. 572, 243–250. https://doi.org/10.1016/j.jhydrol.2019.03.001.

Hao, Z., Hao, F., Singh, V.P., Zhang, X., 2018. Changes in the severity of compound drought and hot extremes over global land areas. Environ. Res. Lett. 13, 124022 https://doi.org/10.1088/1748-9326/aaee96.

Hao, Z., Hao, F., Xia, Y., Feng, S., Sun, C., Zhang, X., Fu, Y., Hao, Y., Zhang, Y., Meng, Y., 2022. Compound droughts and hot extremes: characteristics, drivers, changes, and impacts. Earth Sci. Rev. 235, 104241 https://doi.org/10.1016/j.earscirev.2022.104241.

Hao, Z., Hao, F., Xia, Y., Singh, V.P., Zhang, X., 2019b. A monitoring and prediction system for compound dry and hot events. Environ. Res. Lett. 14, 114034 https://doi.org/10.1088/1748-9326/ab4df5.

He, W., Zhang, J., Yu, X., Chen, S., Luo, J., 2018. Effect of runoff variability and sea level on saltwater intrusion: a case study of nandu River Estuary, China. Water Resour. Res. 54, 9919–9934. https://doi.org/10.1029/2018WR023285.

He, W., Zhou, H., Zhang, J., Xu, H., Liu, C., 2022. Combined effects of runoff increase and sea level rise on the water exchange and saltwater intrusion for an estuary bay in non-flood season. Hydrol. Process. 36, e14727 https://doi.org/10.1002/hyp.14727.

Hoitink, A.J.F., Jay, D.A., 2016. Tidal river dynamics: implications for deltas. Rev. Geophys. 54, 240–272. https://doi.org/10.1002/2015RG000507.

Hu, J., Liu, B., Peng, S., 2019. Forecasting salinity time series using RF and ELM approaches coupled with decomposition techniques. Stoch. Environ. Res. Risk Assess. 33, 1117–1135. https://doi.org/10.1007/s00477-019-01691-1.

Hu, P., Han, J., Li, W., Sun, Z., He, Z., 2018. Numerical investigation of a sandbar formation and evolution in a tide-dominated estuary using a hydro-morphodynamic model. Coast Eng. J. 60, 466–483. https://doi.org/10.1080/21664250.2018.1529263.

Huang, S., Huang, Q., Zhang, H., Chen, Y., Leng, G., 2016. Spatio-temporal changes in precipitation, temperature and their possibly changing relationship: a case study in the Wei River Basin, China. Int. J. Climatol. 36, 1160–1169. https://doi.org/10.1002/joc.4409.

Huang, W., Wang, H., 2021. Drought and intensified agriculture enhanced vegetation growth in the central Pearl River Basin of China. Agric. Water Manag. 256, 107077 https://doi.org/10.1016/j.agwat.2021.107077.

Jia, Z., Li, S., Liu, Q., Jiang, F., Hu, J., 2021. Distribution and partitioning of heavy metals in water and sediments of a typical estuary (Modaomen, South China): the effect of water density stratification associated with salinity. Environ. Pollut. 287, 117277 https://doi.org/10.1016/j.envpol.2021.117277.

Jones, E., van Vliet, M.T.H., 2018. Drought impacts on river salinity in the southern US: implications for water scarcity. Sci. Total Environ. 644, 844–853. https://doi.org/10.1016/j.scitotenv.2018.06.373.

Kang, Y., Guo, E., Wang, Y., Bao, Yulong, Bao, Yuhai, Mandula, N., Runa, A., Gu, X., Jin, L., 2022. Characterisation of compound dry and hot events in Inner Mongolia and their relationship with large-scale circulation patterns. J. Hydrol. 612, 128296 https://doi.org/10.1016/j.jhydrol.2022.128296.

Karl, T.R., 1986. The sensitivity of the palmer drought severity index and palmer's Z-index to their calibration coefficients including potential evapotranspiration. J. Appl. Meteorol. Climatol. 25, 77–86. https://doi.org/10.1175/1520-0450(1986)025<0077:TSOTPD>2.0.CO;2.

Kärnä, T., Baptista, A.M., Lopez, J.E., Turner, P.J., McNeil, C., Sanford, T.B., 2015. Numerical modeling of circulation in high-energy estuaries: a Columbia River estuary benchmark. Ocean Model. 88, 54–71. https://doi.org/10.1016/j.ocemod.2015.01.001.

Leblanc, M., Tweed, S., Van Dijk, A., Timbal, B., 2012. A review of historic and future hydrological changes in the Murray-Darling Basin. Global Planet. Change 80–81, 226–246. https://doi.org/10.1016/j.gloplacha.2011.10.012.

Li, H.W., Li, Y.P., Huang, G.H., Sun, J., 2021a. Quantifying effects of compound dry-hot extremes on vegetation in Xinjiang (China) using a vine-copula conditional probability model. Agric. For. Meteorol. 311, 108658 https://doi.org/10.1016/j.agrformet.2021.108658.

Li, J., Wang, Z., Wu, X., Zscheischler, J., Guo, S., Chen, X., 2021b. A standardized index for assessing sub-monthly compound dry and hot conditions with application in China. Hydrol. Earth Syst. Sci. 25, 1587–1601. https://doi.org/10.5194/hess-25-1587-2021.

Li, X., Yang, F., Zou, H., Wang, S., 2023. Compound Events of Drought and Salt Intrusion in the Greater Bay Area and Adaptation Countermeasures (No. EGU23-12813). Copernicus Meetings. https://doi.org/10.5194/egusphere-egu23-12813. Presented at the EGU23.

Liu, B., Peng, S., Liao, Y., Long, W., 2018. The causes and impacts of water resources crises in the Pearl River Delta. J. Clean. Prod. 177, 413–425. https://doi.org/10.1016/j.jclepro.2017.12.203.

Liu, B., Peng, S., Liao, Y., Wang, H., 2019. The characteristics and causes of increasingly severe saltwater intrusion in Pearl River Estuary. Estuarine. Coastal and Shelf Science 220, 54–63. https://doi.org/10.1016/j.ecss.2019.02.041.

Liu, Z., Törnros, T., Menzel, L., 2016. A probabilistic prediction network for hydrological drought identification and environmental flow assessment: a probabilistic network for drought and flow assessment. Water Resour. Res. 52, 6243–6262. https://doi.org/10.1002/2016WR019106.

Loch, A., Gregg, D., 2018. Salinity management in the murray-darling basin: a transaction cost study. Water Resour. Res. 54, 8813–8827. https://doi.org/10.1029/2018WR022912.

Lu, M., Wang, X., Li, H., Jiao, J.J., Luo, X., Luo, M., Yu, S., Xiao, K., Li, X., Qiu, W., Zheng, C., 2022. Microbial community assembly and co-occurrence relationship in sediments of the river-dominated estuary and the adjacent shelf in the wet season. Environ. Pollut. 308, 119572 https://doi.org/10.1016/j.envpol.2022.119572.

Masih, I., Maskey, S., Mussá, F.E.F., Trambauer, P., 2014. A review of droughts on the African continent: a geospatial and long-term perspective. Hydrol. Earth Syst. Sci. 18, 3635–3649. https://doi.org/10.5194/hess-18-3635-2014.

Merchán, D., Casalí, J., Del Valle de Lersundi, J., Campo-Bescós, M.A., Giménez, R., Preciado, B., Lafarga, A., 2018. Runoff, nutrients, sediment and salt yields in an irrigated watershed in southern Navarre (Spain). Agric. Water Manag. 195, 120–132. https://doi.org/10.1016/j.agwat.2017.10.004.

Mishra, A.K., Singh, V.P., 2010. A review of drought concepts. J. Hydrol. 391, 202–216. https://doi.org/10.1016/j.jhydrol.2010.07.012.

Mitra, S., Srivastava, P., 2021. Comprehensive drought assessment tool for coastal areas, bays, and estuaries: development of a coastal drought index. J. Hydrol. Eng. 26, 04020055 https://doi.org/10.1061/(ASCE)HE.1943-5584.0001968.
Nalbantis, I., Tsakiris, G., 2009. Assessment of hydrological drought revisited. Water Resour. Manag. 23, 881–897. https://doi.org/10.1007/s11269-008-9305-1.
Nienhuis, J.H., Ashton, A.D., Edmonds, D.A., Hoitink, A.J.F., Kettner, A.J., Rowland, J. C., Törnqvist, T.E., 2020. Global-scale human impact on delta morphology has led to net land area gain. Nature 577, 514–518. https://doi.org/10.1038/s41586-019-1905-9.
Ogg, C.M., Kelley, J.A., Wilson, M.A., Tuttle, J.W., Gulley, C.D., Reed, J.M., Sullivan, G. E., 2022. Polygenesis and cementation pathways for plinthic and non-plinthic soils on the Upper Coastal Plain, South Carolina. Geoderma 427, 116130. https://doi.org/10.1016/j.geoderma.2022.116130.
Peters, C.N., Kimsal, C., Frederiks, R.S., Paldor, A., McQuiggan, R., Michael, H.A., 2022. Groundwater pumping causes salinization of coastal streams due to baseflow depletion: analytical framework and application to Savannah River, GA. J. Hydrol. 604, 127238 https://doi.org/10.1016/j.jhydrol.2021.127238.
Phlips, E.J., Badylak, S., Mathews, A.L., Milbrandt, E.C., Montefiore, L.R., Morrison, E.S., Nelson, N., Stelling, B., 2023. Algal blooms in a river-dominated estuary and nearshore region of Florida, USA: the influence of regulated discharges from water control structures on hydrologic and nutrient conditions. Hydrobiologia. https://doi.org/10.1007/s10750-022-05135-w.
Qiu, J., Liu, B., Yang, F., Wang, X., He, X., 2022. Quantitative stress test of compound coastal-fluvial floods in China's Pearl River delta. Earth's Future 10, e2021EF002638. https://doi.org/10.1029/2021EF002638.
Rijnsburger, S., Flores, R.P., Pietrzak, J.D., Lamb, K.G., Jones, N.L., Horner-Devine, A.R., Souza, A.J., 2021. Observations of multiple internal wave packets in a tidal river plume. J. Geophys. Res.: Oceans 126, e2020JC016575. https://doi.org/10.1029/2020JC016575.
Romaní, A.M., Sabater, S., Muñoz, I., 2010. The physical framework and historic human influences in the Ebro river. In: Barceló, D., Petrovic, M. (Eds.), The Ebro River Basin, the Handbook of Environmental Chemistry. Springer Berlin Heidelberg, Berlin, Heidelberg, pp. 1–20. https://doi.org/10.1007/698_2010_66.
Shao, S., Zhang, H., Singh, V.P., Ding, H., Zhang, J., Wu, Y., 2022. Nonstationary analysis of hydrological drought index in a coupled human-water system: application of the GAMLSS with meteorological and anthropogenic covariates in the Wuding River basin, China. J. Hydrol. 608, 127692 https://doi.org/10.1016/j.jhydrol.2022.127692.
Shen, Y., Jia, H., Li, C., Tang, J., 2018. Numerical simulation of saltwater intrusion and storm surge effects of reclamation in Pearl River Estuary, China. Appl. Ocean Res. 79, 101–112. https://doi.org/10.1016/j.apor.2018.07.013.
Shi, X., Qin, T., Nie, H., Weng, B., He, S., 2019. Changes in major global river discharges directed into the ocean. Int. J. Environ. Res. Publ. Health 16, 1469. https://doi.org/10.3390/ijerph16081469.
Shukla, S., Wood, A.W., 2008. Use of a standardized runoff index for characterizing hydrologic drought. Geophys. Res. Lett. 35 https://doi.org/10.1029/2007GL032487.
Steyl, G., Dennis, I., 2010. Review of coastal-area aquifers in Africa. Hydrogeol. J. 18, 217–225. https://doi.org/10.1007/s10040-009-0545-9.
Svoboda, M., LeComte, D., Hayes, M., Heim, R., Gleason, K., Angel, J., Rippey, B., Tinker, R., Palecki, M., Stooksbury, D., Miskus, D., Stephens, S., 2002. The drought monitor. Bull. Am. Meteorol. Soc. 83, 1181–1190. https://doi.org/10.1175/1520-0477-83.8.1181.
Tan, Xuejin, Liu, B., Tan, Xuezhi, 2020. Global changes in baseflow under the impacts of changing climate and vegetation. Water Resour. Res. 56 https://doi.org/10.1029/2020WR027349.
Tan, Xuejin, Liu, B., Tan, Xuezhi, Chen, X., 2022. Long-Term water imbalances of watersheds resulting from biases in hydroclimatic data sets for water budget analyses. Water Resour. Res. 58 https://doi.org/10.1029/2021WR031209.
Thom, B., Rocheta, E., Steinfeld, C., Harvey, N., Pittock, J., Cowell, P., 2020. The role of coastal processes in the management of the mouth of the River Murray, Australia: present and future challenges. River Res. Appl. 36, 656–667. https://doi.org/10.1002/rra.3551.
Thorslund, J., Bierkens, M.F.P., Oude Essink, G.H.P., Sutanudjaja, E.H., van Vliet, M.T. H., 2021. Common irrigation drivers of freshwater salinisation in river basins worldwide. Nat. Commun. 12, 4232. https://doi.org/10.1038/s41467-021-24281-8.
Valiya Veettil, A., Mishra, A.k., 2020. Multiscale hydrological drought analysis: role of climate, catchment and morphological variables and associated thresholds. J. Hydrol. 582, 124533 https://doi.org/10.1016/j.jhydrol.2019.124533.
Verbrugge, L.N.H., Schipper, A.M., Huijbregts, M.A.J., Van der Velde, G., Leuven, R.S.E. W., 2012. Sensitivity of native and non-native mollusc species to changing river water temperature and salinity. Biol. Invasions 14, 1187–1199. https://doi.org/10.1007/s10530-011-0148-y.
Vicente-Serrano, S.M., López-Moreno, J.I., Beguería, S., Lorenzo-Lacruz, J., Azorin-Molina, C., Morán-Tejeda, E., 2012. Accurate computation of a streamflow drought index. J. Hydrol. Eng. 17, 318–332. https://doi.org/10.1061/(ASCE)HE.1943-5584.0000433.
Vicente-Serrano, S.M., Zabalza-Martínez, J., Borràs, G., López-Moreno, J.I., Pla, E., Pascual, D., Savé, R., Biel, C., Funes, I., Martín-Hernández, N., Peña-Gallardo, M., Beguería, S., Tomas-Burguera, M., 2017. Effect of reservoirs on streamflow and river regimes in a heavily regulated river basin of Northeast Spain. In: CATENA, Geoecology in Mediterranean Mountain Areas. Tribute to Professor José María García Ruiz, vol. 149, pp. 727–741. https://doi.org/10.1016/j.catena.2016.03.042.
Wada, Y., Beek, L.P.H. van, Wanders, N., Bierkens, M.F.P., 2013. Human water consumption intensifies hydrological drought worldwide. Environ. Res. Lett. 8, 034036 https://doi.org/10.1088/1748-9326/8/3/034036.
Wang, F., Wang, Z., Yang, H., Di, D., Zhao, Y., Liang, Q., 2020a. A new copula-based standardized precipitation evapotranspiration streamflow index for drought monitoring. J. Hydrol. 585, 124793 https://doi.org/10.1016/j.jhydrol.2020.124793.
Wang, F., Wang, Z., Yang, H., Di, D., Zhao, Y., Liang, Q., Hussain, Z., 2020b. Comprehensive evaluation of hydrological drought and its relationships with meteorological drought in the Yellow River basin, China. J. Hydrol. 584, 124751 https://doi.org/10.1016/j.jhydrol.2020.124751.
Wang, H., Dai, Z., Trettin, C.C., Krauss, K.W., Noe, G.B., Burton, A.J., Stagg, C.L., Ward, E.J., 2022c. Modeling impacts of drought-induced salinity intrusion on carbon dynamics in tidal freshwater forested wetlands. Ecol. Appl. 32, e2700 https://doi.org/10.1002/eap.2700.
Wang, J., Hong, B., Gong, W., 2022d. Study of an abnormally strong saltwater intrusion in the Humen Channel of the Pearl River estuary. Anthropocene Coasts 5, 7. https://doi.org/10.1007/s44218-022-00008-0.
Wang, T., Tu, X., Singh, V.P., Chen, X., Lin, K., 2022a. A composite index coupling five key elements of water cycle for drought analysis in Pearl River basin, China. J. Environ. Manag. 320, 115813 https://doi.org/10.1016/j.jenvman.2022.115813.
Wang, T., Tu, X., Singh, V.P., Chen, X., Lin, K., 2021a. Global data assessment and analysis of drought characteristics based on CMIP6. J. Hydrol. 596, 126091 https://doi.org/10.1016/j.jhydrol.2021.126091.
Wang, T., Tu, X., Singh, V.P., Chen, X., Lin, K., Lai, R., Zhou, Z., 2022b. Socioeconomic drought analysis by standardized water supply and demand index under changing environment. J. Clean. Prod. 347, 131248 https://doi.org/10.1016/j.jclepro.2022.131248.
Wang, T., Tu, X., Singh, V.P., Chen, X., Lin, K., Zhou, Z., Zhu, J., 2023. A CMIP6-based framework for propagation from meteorological and hydrological droughts to socioeconomic drought. J. Hydrol. 623, 129782 https://doi.org/10.1016/j.jhydrol.2023.129782.
Wang, W., Zhang, Y., Guo, B., Ji, M., Xu, Y., 2021b. Compound droughts and heatwaves over the Huai River Basin of China: from a perspective of the magnitude index. J. Hydrometeorol. https://doi.org/10.1175/JHM-D-20-0305.1.
Wang, Y., Duan, L., Liu, T., Li, J., Feng, P., 2020c. A Non-stationary Standardized Streamflow Index for hydrological drought using climate and human-induced indices as covariates. Sci. Total Environ. 699, 134278 https://doi.org/10.1016/j.scitotenv.2019.134278.
Wei, X., Williams, M.E., Brown, J.M., Thorne, P.D., Amoudry, L.O., 2022. Salt intrusion as a function of estuary length in periodically weakly stratified estuaries. Geophys. Res. Lett. 49 https://doi.org/10.1029/2022GL099082 e2022GL099082.
Werner, A.D., 2010. A review of seawater intrusion and its management in Australia. Hydrogeol. J. 18, 281–285. https://doi.org/10.1007/s10040-009-0465-8.
Wu, H., Su, X., Singh, V.P., 2021. Blended dry and hot events index for monitoring dry-hot events over global land areas. Geophys. Res. Lett. 48 https://doi.org/10.1029/2021GL096181.
Wu, J., Chen, X., Yao, H., Liu, Z., Zhang, D., 2018. Hydrological drought instantaneous propagation speed based on the variable motion relationship of speed-time process. Water Resour. Res. 54, 9549–9565. https://doi.org/10.1029/2018WR023120.
Wu, J., Chen, X., Yu, Z., Yao, H., Li, W., Zhang, D., 2019. Assessing the impact of human regulations on hydrological drought development and recovery based on a 'simulated-observed' comparison of the SWAT model. J. Hydrol. 577, 123990 https://doi.org/10.1016/j.jhydrol.2019.123990.
Wu, J., Yao, H., Chen, X., Wang, G., Bai, X., Zhang, D., 2022. A framework for assessing compound drought events from a drought propagation perspective. J. Hydrol. 604, 127228 https://doi.org/10.1016/j.jhydrol.2021.127228.
Wu, X., Hao, Z., Hao, F., Singh, V.P., Zhang, X., 2019a. Dry-hot magnitude index: a joint indicator for compound event analysis. Environ. Res. Lett. 14, 064017 https://doi.org/10.1088/1748-9326/ab1ec7.
Wu, X., Hao, Z., Hao, F., Zhang, X., 2019b. Variations of compound precipitation and temperature extremes in China during 1961–2014. Sci. Total Environ. 663, 731–737. https://doi.org/10.1016/j.scitotenv.2019.01.366.
Wu, X., Hao, Z., Zhang, X., Li, C., Hao, F., 2020. Evaluation of severity changes of compound dry and hot events in China based on a multivariate multi-index approach. J. Hydrol. 583, 124580 https://doi.org/10.1016/j.jhydrol.2020.124580.
Yu, R., Zhai, P., 2020. Changes in compound drought and hot extreme events in summer over populated eastern China. Weather Clim. Extrem. 30, 100295 https://doi.org/10.1016/j.wace.2020.100295.
Zhang, D., Zhang, Q., Qiu, J., Bai, P., Liang, K., Li, X., 2018. Intensification of hydrological drought due to human activity in the middle reaches of the Yangtze River, China. Sci. Total Environ. 637, 1432–1442. https://doi.org/10.1016/j.scitotenv.2018.05.121. –638.
Zhang, T., Su, X., Feng, K., 2021. The development of a novel nonstationary meteorological and hydrological drought index using the climatic and anthropogenic indices as covariates. Sci. Total Environ. 786, 147385 https://doi.org/10.1016/j.scitotenv.2021.147385.
Zhang, W., Luo, M., Gao, S., Chen, W., Hari, V., Khouakhi, A., 2021. Compound hydrometeorological extremes: drivers, mechanisms and methods. Front. Earth Sci. 9.
Zhang, Y., Yang, X., Chen, C., 2021. Substantial decrease in concurrent meteorological droughts and consecutive cold events in Huai River Basin, China. Int. J. Climatol. 41, 6065–6083. https://doi.org/10.1002/joc.7168.
Zhou, F., Liu, B., Duan, K., 2020. Coupling wavelet transform and artificial neural network for forecasting estuarine salinity. J. Hydrol. 588, 125127 https://doi.org/10.1016/j.jhydrol.2020.125127.
Zhou, P., Liu, Z., 2018. Likelihood of concurrent climate extremes and variations over China. Environ. Res. Lett. 13, 094023 https://doi.org/10.1088/1748-9326/aade9e.

Zhou, Z., Shi, H., Fu, Q., Ding, Y., Li, T., Wang, Y., Liu, S., 2021. Characteristics of propagation from meteorological drought to hydrological drought in the Pearl River basin. JGR Atmospheres 126. https://doi.org/10.1029/2020JD033959.

Zscheischler, J., Martius, O., Westra, S., Bevacqua, E., Raymond, C., Horton, R.M., van den Hurk, B., AghaKouchak, A., Jézéquel, A., Mahecha, M.D., Maraun, D., Ramos, A. M., Ridder, N.N., Thiery, W., Vignotto, E., 2020. A typology of compound weather and climate events. Nat. Rev. Earth Environ. 1, 333–347. https://doi.org/10.1038/s43017-020-0060-z.

Zscheischler, J., Seneviratne, S.I., 2017. Dependence of drivers affects risks associated with compound events. Sci. Adv. 3, e1700263 https://doi.org/10.1126/sciadv.1700263.